CHALMERS
UNIVERSITY OF TECHNOLOGY

Optimization for Energy Efficient Cooperative Adaptive Cruise Control

A Moving Horizon Predictive Controller for Truck Platoons

Master's thesis in Systems, Control and Mechatronics

MAMADOU DIABY
ALAADDIN SORKATI

Department of Signals and Systems
CHALMERS UNIVERSITY OF TECHNOLOGY
Gothenburg, Sweden 2016

Master's thesis EX054/2016

Optimization for Energy Efficient Cooperative Adaptive Cruise Control

A Moving Horizon Predictive Controller for Truck Platoons

MAMADOU DIABY
ALAADDIN SORKATI

CHALMERS
UNIVERSITY OF TECHNOLOGY

Department of Signals and Systems
Automatic Control Group
Chalmers University of Technology
Gothenburg, Sweden 2016

Optimization For Energy Efficient Cooperative Adaptive Cruise Control
A Moving Horizon Predictive Controller for Truck Platoons
MAMADOU DIABY, ALAADDIN SORKATI

Supervisor: Martin Sanfridson, Vehicle Dynamics and Active Safety, Volvo GTT
Supervisor & Examiner: Nikolce Murgovski, Department of Signals and Systems

Master's Thesis EX054/2016
Department of Signals and Systems
Automatic Control Group
Chalmers University of Technology
SE-412 96 Gothenburg
Telephone +46 31 772 1000

Cover: Volvo self-driving truck platoon in the European Truck Platooning Challenge

Typeset in LaTeX
Printed by Chalmers Reproservice
Gothenburg, Sweden 2016

Optimization For Energy Efficient Cooperative Adaptive Cruise Control
A Moving Horizon Predictive Controller for Truck Platoons
MAMADOU DIABY, ALAADDIN SORKATI
Department of Signals and Systems
Chalmers University of Technology

Abstract

In the recent years, substantial amount of researches have been centred around automated driving both in academia and in the automotive industries. One of the main target of those researches is to reduce energy consumption and consequently mitigate the effect of fuel emissions. Tremendous fuel saving can be achieved by taking advantage of the topographic information and by employing techniques to reduce air drag.

This thesis presents a method for minimizing fuel consumption of truck platoons travelling on hilly roads with respect to both the topography and air drag. The problem is formulated as a convex quadratic programming problem that, in a moving horizon approach, optimizes vehicles' velocities, while not violating the minimum inter-vehicular distance constraint. Emphasis is put on a homogeneous three-vehicle platoon and real-time solvers are generated using FORCES Pro to solve the problem centrally and in a decoupled approach. The proposed control scheme is computationally efficient, while the results show fuel saving of up to 5.6% for a three vehicle platoon travelling on the *Borås-Landvetter-Borås* drive cycle depending on the vehicles' weights.

Keywords: quadratic programming, model predictive control (MPC), vehicle platoon, fuel optimization, headway time, predictive cruise controller

Acknowledgements

All praises are due to *Allah* to him we owe our success.

We would first like to express our gratitude to Volvo Group Trucks Technology for giving us the opportunity to carry out our thesis work at Volvo.
We would specially like to thank and show appreciation to our supervisors Martin Sanfridson and Nikolce Murgovski. Their continuous support and guidance from the early to the latter stage of the project was key to reaching this far. Our special thanks also goes to Olof Lindgärde for his valuable inputs.
We would also like to thank the Swedish Institute (SI) for funding our studies at Chalmers and for the opportunity to be part of the network for future global leaders. Being part of this network has truly been rewarding and inspiring both personally and academically.

Last but not least, we would like to extend our gratitude and appreciation to our friends and families for their continuous support and motivation throughout the years.

Mamadou Diaby and Aladdin Sorkati
Gothenburg, June 2016

Contents

List of Figures

List of Tables

1

Introduction

Reducing fuel consumption has always been a major concern for the automotive industry due to its environmental and economical impacts as well as regulatory demands. The environmental and economical issues and the rising fuel prices stimulate researchers to develop methods in order to overcome these challenges.

In recent years, there has been an increasing interest in the development of automated vehicular control strategies. The adaptive cruise control (ACC) is one of the longitudinal control schemes used to control the vehicle's speed in order to keep a safe gap from vehicles ahead with help of on-board sensors e.g. radar or laser. The ACC employs the lead vehicle's information; it therefore needs to capture a change in its movement to decide whether to speed up or slow down. Since there is a delay in capturing this information, there is a limit to the gap that can be technically maintained.

By improving ACC to the cooperative ACC (CACC), in which all the vehicles share their information, e.g. position, velocities and acceleration via vehicle to vehicle (V2V) communication, the following vehicle is able to respond faster. This improvement enables to link more than one vehicle in a stable string. Such strings, as shown in Figure 1.1, where vehicles maintain a relatively small inter-vehicle distance is known as a platoon.

Figure 1.1: A platoon of N vehicles where $d_{i,i+1}$ denotes the bumper to bumper distance between vehicles i and $i+1$.

Having heavy-duty vehicles (HDV), with large frontal areas, as lead vehicles in platoons could reduce the air resistance force experienced by the succeeding vehicles. This reduction will downscale the torque required to drive the vehicles at a certain speed which, in turn, decreases the fuel consumption. The cooperative control in which the vehicles maintain a relatively small inter-distance is known as platooning.

Another approach to improve the fuel-economy is to utilize the knowledge of upcoming topography in order to benefit from the vehicle's kinetic and potential energy storage. Planning velocity with respect to the future topography may lead to a varying velocity trajectory depending on the terrain.

In this thesis, both the topography utilization and platooning are combined in order to minimize the fuel consumption of a truck platoon travelling in hilly terrain.

1.1 Background

Many studies have been carried out regarding optimal energy management. In [1, 2, 3], the aerodynamic drag reduction is used to maximize the energy efficiency while a constant gap is kept between the vehicles. Although the platoon benefits from the air drag reduction, constantly maintaining a fixed gap between the platoon participants results in frequent usage of the brakes especially at downhill sections.

E. Hellström et al. in [4, 5] used an on-board slope database and GPS unit to extract the data about the road topography ahead. They devised a dynamic programming algorithm [6] in a model predictive control (MPC) scheme [7] to feed the cruise controllers with new set points continuously. The obtained fuel consumption reduction constrained to the trip time is about 3.5% within a distance of 120 km. However, the computation time grows exponentially with the number of system states, which limits the possibility of applying the proposed method on a platoon of several vehicles [8].

Olof Lindgärde et al., in the CONVENIENT project [9], in affiliation with Volvo Group Trucks Technology, developed a model-based optimal control strategy that uses predictive information from the e-Horizon system to optimize fuel consumption for hybrid long-haul tractor and semi-trailer combinations. They also made use of adaptive aerodynamics to reduce fuel consumption by automatically setting an optimal angle for both a roof deflector and a side deflector. After implementation on a truck, namely the Volvo 6x2 tractor, test results show that the total fuel saving of the predictive controller is close to 0.5% and the reduction of mechanical work by the alternator is 19%. However, Olof Lindgärde et al. did not consider vehicle platoons.

In this thesis, two strategies of energy management for platoons are investigated; namely a centralized approach where there is cooperation between the platoon participants and a decoupled approach, referred to as 'greedy', where each vehicle optimizes its own fuel consumption without considering what is optimal for the other participants. In both strategies, the controllers act as supervisory controllers, that is to say they provide optimal reference trajectories to existing local controllers which in turn generate desired input signals for the vehicles in the platoon.
Figures 1.2 and 1.3 show a systematic layout for the centralized and the greedy method respectively.

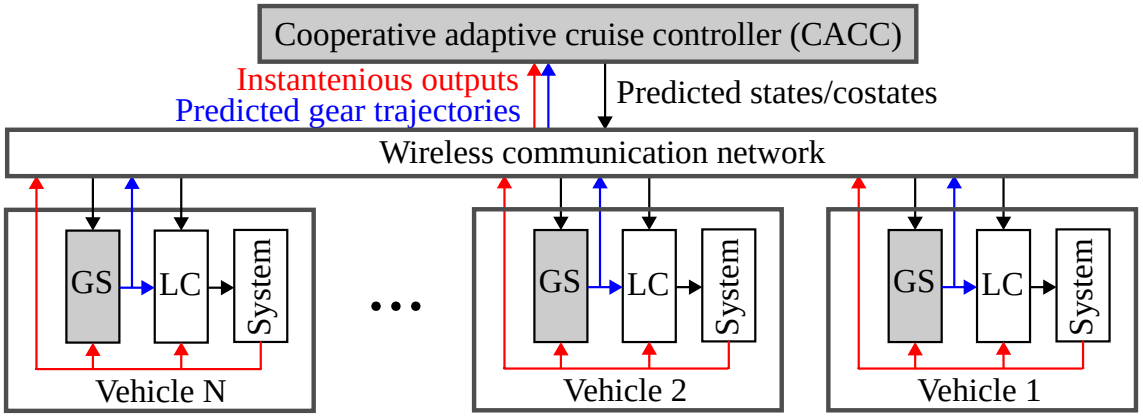

Figure 1.2: Centralized cooperative adaptive cruise controller (CACC). The CACC generates state trajectories for all the vehicles over the prediction horizon. The predicted trajectories are used as inputs to the local controllers (LC) and the gear selector (GS) [8].

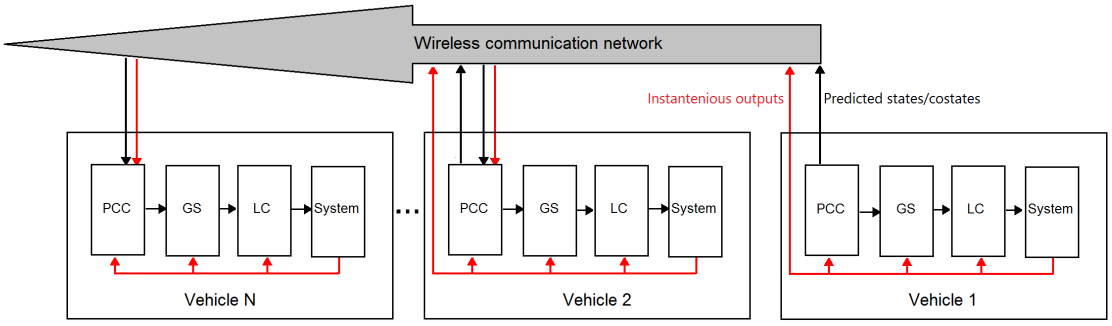

Figure 1.3: The greedy method. Each vehicle has its own predictive cruise controller; vehicle 1 bases its speed profile on the topography whereas subsequent vehicles base their speed on the topography and on the speed profiles of up to two vehicles ahead that they receive via V2V communication.

In the centralized method, the controller, also referred to as cooperative adaptive cruise controller(CACC) in Figure 1.2, controls the platoon participants in a centralized manner; i.e the controller minimizes the fuel consumption for the platoon. This controller also requires private information sharing, such as weights, power limits, etc., via V2V communication between the platoon participants.

The greedy method, as shown in Figure 1.3, is a decoupled version of the CACC where each vehicle has its own predictive cruise controller (PCC). Each of the vehicles communicates backwards its planned speed and or time trajectories over the horizon. The lead vehicle plans its speed based on the upcoming topography and the following vehicles plan their speed based on both the topography and the planned trajectories of the two vehicles in front of them. In this method, private information such as masses and engine limits needs not be shared. Information sent via V2V is limited to initial positions, initial speeds and planned speeds or time trajectories over the horizon. The greedy method consist of solving a number of relatively

small optimization tasks whereas in the centralized method one large optimization problem is solved.

1.2 Aim

The aim of this thesis is to, in a moving horizon approach, optimize fuel saving for a truck platoon travelling in a hilly terrain with respect to both topography and air drag. The thesis is largely based on work done in [8]. An additional goal of this thesis is code generation for real-time solvers for the optimization problems.

1.3 Methods

Model predictive control (MPC) is a central element of the optimization tasks. Therefore a mathematical description of each of the vehicles will first be modeled; from the individual vehicle models, the platoon model can be found depending on the number of the vehicles in the platoon.

Throughout the thesis, only convex and quadratic optimization problems are considered simply because local optima for such problems are also global ones [10]. Hence non-convex components, be they constraints or part of the cost function, are convexified.

Only linear and discrete domain MPC are considered in the thesis. Hence the mathematical model of the platoon is linearized and discretized continuously at every sampling instant prior to solving for the optimal trajectories.

The predictive controllers are intended to provide optimal references to the existing adaptive cruise controller (ACC). The predictive controllers use the topography, a feedback from the vehicles as well as a desired cruising speed to generate the reference trajectories for the lower layer controller ACC. The references for the ACC include both a speed for the lead vehicle and a gap for the following vehicles.

FORCES Pro is used to generate C code for real-time solvers. The optimal trajectories from the optimization problems, be they speed or gap, are provided, in a moving horizon approach, to their respective lower layer controllers and the platoon is simulated in SIMULINK to evaluate its behavior.

Two types of predictive control schemes are presented and compared to each other. The cooperative predictive controller optimizes the fuel consumption for the entire platoon whereas in the greedy method, each of the platoon participants optimizes their own fuel consumption without considering what is optimal for the platoon. The fuel consumptions and the computation times of the two control strategies are also analyzed. A simple platoon controller that maintains a constant speed for the lead vehicle and a constant gap for the following vehicles is used as a baseline for comparison and evaluation.

1.4 Delimitations

The focus of this thesis is on longitudinal control. Hence lateral control is beyond the scope. Additionally, the lower layer controllers, i.e. speed and gap controllers, are assumed to exist; their design and implementation are not presented. The number of vehicles in the platoon is also assumed to be constant and surrounding traffic, external to the platoon, is not modeled.

1.5 Thesis outline

Chapter 2 describes the vehicle model for longitudinal dynamics. Additionally, the drive cycles used as test cases are introduced and a conceptual formulation of the problem is provided at the end of the chapter.

Chapter 3 introduces the two control strategies adopted in the thesis. This chapter also discusses necessary linearizations, approximations and variable changes needed to keep the problem, for both strategies, quadratic and convex. Mathematical formulations of the two controller architectures are presented at the end of the chapter together with a brief introduction of the tool used for code generation.

Open loop solutions, based on a test drive cycle, are elaborated in Chapter 4 whereas Chapter 5 discusses the closed loop GSP simulation results and the fuel consumptions for both a single vehicle and a three-vehicle platoon. In the two final chapters, Chapter 6 and Chapter 7, the conclusions of the thesis are stated and some future improvements are suggested.

2

System Description

This chapter describes both the engine model and the non-linear vehicle model. The air drag reduction functions are also presented. Note that, throughout the thesis, sampling and discretization are performed in space domain instead of the conventional time domain. The road profiles used as test cases are introduced at the end of the chapter. The chapter is then concluded with a conceptual formulation of the energy management problem.

2.1 Longitudinal vehicle dynamics

If one considers the vehicle V_i, occupying position i in the platoon, as point mass then the equation of its longitudinal motion in continuous-space domain, according to Newton's second law of motion, can be written as

$$\begin{aligned} m_i\sigma_i v_i'(s)v_i(s) =& F_{Ei}(s) - F_{bi}(s) - F_{airi}(v_i) - m_i g(\sin\alpha(s) + c_r\cos\alpha(s)) - \\ & - \frac{P_{xi}}{v_i(s)} \end{aligned} \tag{2.1}$$

where s is the position along the route. m_i, σ_i are the vehicle mass and the rotational mass ratio respectively. F_{Ei}, F_{bi},F_{airi} are the force attained at wheel side from the engine, the braking force and the air resistance respectively. α is the road gradient, g the gravity and c_r the rolling resistance coefficient. The term P_{xi} reflects the power consumption due to auxiliary devices.

The term v_i' in (2.1) is defined as

$$v_i' = \frac{dv_i}{ds} \tag{2.2}$$

and it represents the space derivative of the velocity. Hence the term $v_i'v_i$ is defined as

$$v_i'v_i = \frac{dv_i}{ds}\frac{ds}{dt} = \frac{dv_i}{dt} \tag{2.3}$$

and is the longitudinal acceleration of the vehicle V_i. Consequently, this implies that the travel time of the vehicle V_i is a state governed by:

$$t_i'(s) = \frac{1}{v_i(s)}. \tag{2.4}$$

The product $m_i\sigma_i$ in (2.1) represents the equivalent vehicle mass, that is, the actual vehicle mass and terms reflecting the inertia of rotational components. This product will be referred to as the equivalent vehicle mass from this point on; and is denoted by m_{ei}.

The sum $m_i g(\sin\alpha(s) + c_r \cos\alpha(s))$ depends on the slope of the road and is a known constant at position s; to make the equations more compact, it will now be referred to as $F_{si}(s)$. A compact version of (2.1) can be written as

$$m_{ei} v_i'(s) v_i(s) = F_{Ei}(s) - F_{bi}(s) - F_{airi}(v_i) - F_{si}(s) - \frac{P_{xi}}{v_i(s)}. \tag{2.5}$$

From (2.5) and (2.4), there are two state variables t and v, and two control signals, F_E and F_b, for each of the vehicles in the platoon.

The nominal air resistance force exhibited in the absence of neighbouring vehicles, for a single vehicle V_i, is given by

$$F^0_{airi}(v_i) = \frac{\rho_a c_d A_f v_i^2(s)}{2} \tag{2.6}$$

where A_f is the frontal area of the vehicle, c_d the aerodynamic drag coefficient and ρ_a the air density. Note that the nominal force is subject to reductions when surrounding vehicles are present. The reduction functions are introduced and discussed thoroughly in Section 2.3

2.2 Engine model

The engine model used throughout the project is adopted from [8]. The fuel mass rate of the engine, μ, is found by fitting a function to measurements of both the engine torque T_E, and its angular velocity ω_E. The measurements and the fitted functions are shown in Figure 2.1.

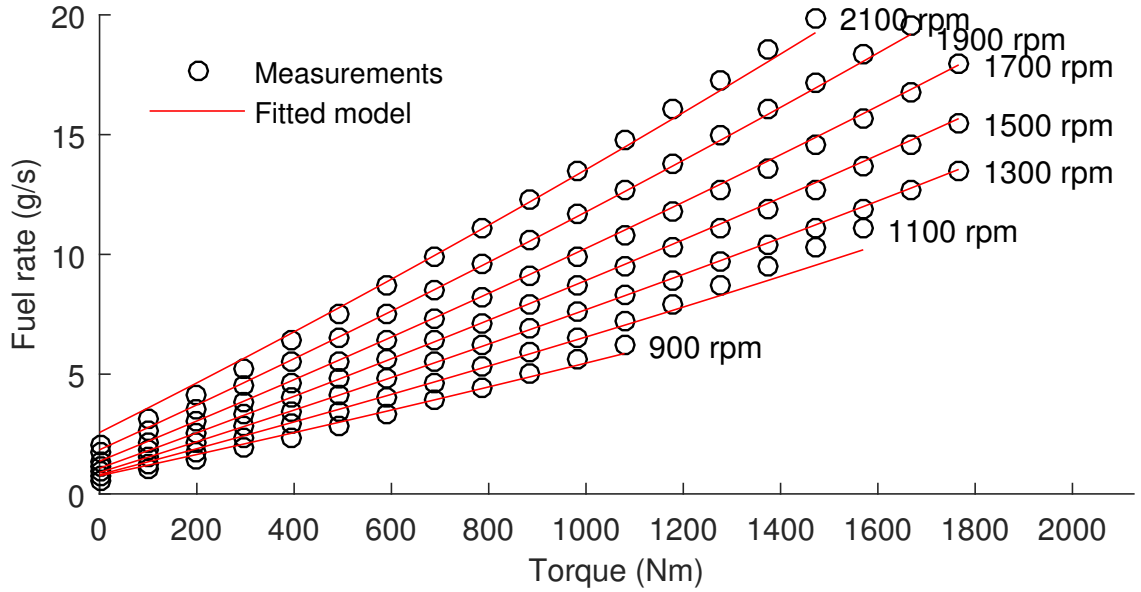

Figure 2.1: Fuel mass rate measured at steady state and fitted model for a set of engine speed values [8].

As can be observed in Figure 2.1, the mass flow is linear at lower torques whereas it tends to be curved at higher torques. As such, a second order polynominal is used for the torque dependency while higher order terms are introduced for the dependency on the angular velocity. The adopted engine model for a vehicle in position i in the platoon is thus given by

$$\mu_i(\omega_{Ei}, T_{Ei}) = a_0 + \omega_{Ei}(s)\left(\sum_{j=1}^{2} a_j T_{Ei}^j(s) + \sum_{j=3}^{5} a_j \omega_{Ei}^{j-1}(s)\right) \tag{2.7}$$

where $a_j \geq 0$, $j = 0, \ldots 5$, and a_0 represents the fuel flow when the engine is idling. Note that these coefficient are not necessarily the same for all the vehicles.

The following relations also hold respectively between the engine speed and torque, ω_{Ei}, T_{Ei} and the vehicle speed and the the force attained at wheel side from the engine, v_i, F_{Ei}:

$$v_i(s) = \omega_{Ei}(s) r(\gamma), \qquad F_{Ei} = T_{Ei}(s)\eta / r(\gamma), \tag{2.8}$$

where γ refers to the selected gear and r is the product of radius of the wheel with the gearing ratio, from the engine to the wheels, in meters. η represents the efficiency from the engine to the wheels, i.e. the transmission efficiency. Assuming that there

is no wheel slip, the maximum longitudinal force that the engine can supply will vary depending on the engine torque, the selected gear and vehicle speed. These limits on the engine force are addressed in Section 3.7.2. Since the objective is to minimize fuel consumption, the cost function will include a simplified version of the fuel flow, μ, given in (2.7).

2.3 Air drag reduction

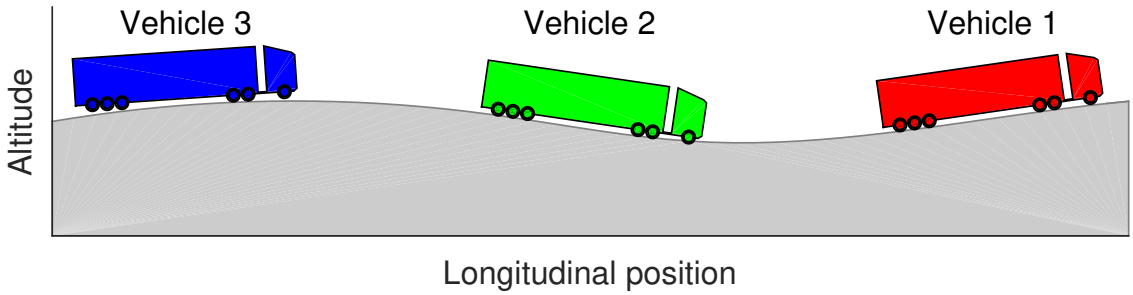

Figure 2.2: Platoon formation of 3 vehicles travelling in hilly terrain

If vehicles are driving in a platoon formation, then they are subject to a reduction in aerodynamic force depending on how close they are to their neighboring vehicles. The extent to which this reduction is experienced varies depending on the vehicle geometry, speed , inter-vehicle distance and other environmental factors such as side wind which changes according to the heading of the road.

By neglecting potential sources of uncertainty in the air drag model, simplified models suitable for the control objective are adopted. The models are all found by fitting functions to the measurements of the drag reduction with respect to the inter-vehicle distance from 2.5 m to 100 m as shown Figure 2.3.

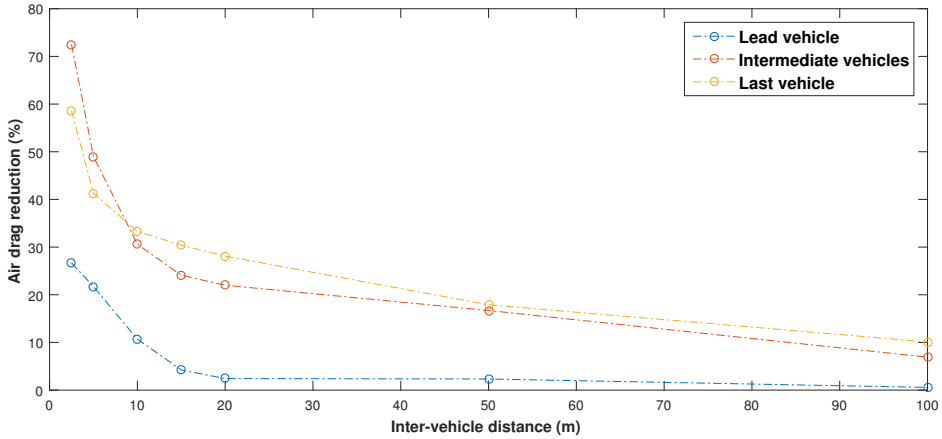

Figure 2.3: Measurement data of the drag reduction as a function of the bumper-to-bumper distance courtesy of AB Volvo.

In the presence of surrounding vehicles the air drag force is found as

$$F_{airi}(v_i, d_{ji}) = F^0_{airi}(v_i)\left(1 - \sum_j f_d(d_{ji}(s))\right) \tag{2.9}$$

with $j = \{i-1, i-2\} \cap \{1, \ldots, N\}$ and $f_d(d_{ji}(s))$ the reduction function fitted to the data given in Figure 2.3.

The model given in (2.9) concentrates on two different contributions to the aerodynamic drag reduction; namely, the contribution from the pull of the two closest vehicles in front.

The drag reduction is a function of the inter-vehicle distance d_{ji}, i.e. the distance between vehicle V_i and V_j; if one considers x_i and x_j to be the longitudinal positions of vehicles V_i and V_j, the inter-distance d_{ji} can be computed as

$$d_{ji} = (x_j(s) - x_i(s)) - L_{ji} \tag{2.10}$$

where L_{ji} is a constant parameter that depends on the length of the vehicles V_i and V_j. If for instance the vehicles have the same length L, then this parameter is simply L. Note that the subscript j can take up to two values, i.e the indices of the two vehicles ahead, $i-1$, and $i-2$.

The reduction function in (2.9), obtained by fitting functions to the measurement data shown in Figure 2.3, is the inverse polynominal given by

$$f_d(d_{ji}) = \frac{1}{\left(c_{0ji} + c_{1ji} d_{ji}(s)\right)^2} \tag{2.11}$$

where c_{0ji}, c_{1ji} are coefficients obtained from the least squares fit to the measurement data. An inverse polynominal function, without the raise to the power of 2, has also been previously proposed in [11]. The drag reduction function given (2.11) was also used in [8].

2.4 Hill profiles

Since the energy management problem is centered around a pre-defined topography information, two different road profiles are considered for the evaluation and analysis of the control strategies presented in Chapter 3. One of the drive cycles is based on measurements courtesy of AB Volvo, i.e. the *Borås-Landvetter-Borås* (BLB) and the short 20km drive cycle is a constructed drive cycle adopted from [8]. The various drive cycles, sampled at 80 meters, are depicted in Figure 2.4. Since the Borås-Landvetter-Borås cycle is based on actual measurements, and also because it represents a typical Swedish highway, it is used in the closed loop MPC simulations presented in Chapter 5. The short 20 kilometer test cycle is used for evaluations in the open loop simulations in Chapter 4.

Figure 2.4: Road profiles used as test cases sampled at 80 meters

2.5 Problem formulation

Given a road profile, the fuel minimization problem consists of finding the fuel-optimal velocity for the lead vehicle and the fuel-optimal velocity and gap for the following vehicles over the driving cycle; and then feeding those optimal trajectories, be they velocities or gaps, as references to the existing lower layer controllers. In lieu of solving the problem for the entire driving cycle, a moving horizon predictive control strategy is adopted where the optimization is solved in parts over the driving cycle.

Given a defined driving cycle and a prediction horizon of $[s_0\ s_f]$, the energy management problem is then formulated as follow:

$$\min_{\omega_E, T_E} \sum_{i=1}^{N} \mu_i(\omega_{Ei}, T_{Ei}) + P_{ci} \tag{2.12}$$

subject to:

1. $m_{ei} v_i'(s) v_i(s) = F_{Ei}(s) - F_{bi}(s) - F_{airi}(v_i) - F_{si}(s) - \frac{P_{xi}}{v_i(s)},\ \forall i \in [1\ N], \forall s \in [s_0\ s_f]$
2. Vehicles limits (all vehicles)
3. Safety constraints

Note that the term P_{ci}, in (2.12), represents other performance cost terms that are presented in Section 3.7.3. Additionally, the horizon starts from the position of the lead vehicle in the platoon, that is to say, the control of the following vehicles prior to reaching the position of the lead vehicle is outside the thesis scope; the consequences of this assumption are addressed in Chapter 5.

In this thesis, the problem defined above is solved in both a holistic approach where the vehicles in the platoon cooperate towards a fuel-optimal solution for the entire platoon, and a greedy approach where each vehicles optimizes for itself but communicates its optimal trajectories over the horizon backwards.

3

The two predictive controllers

In this chapter, the two approaches are introduced to solve the problem defined in Section 2.5. Additionally, necessary linearizations, simplifications and variable changes, that are needed in both approaches not only to reduce the problem complexity but also to keep it quadratic and convex, are presented and discussed. Furthermore, the various limits on the optimization variables are introduced; the two approaches are then mathematically presented and the main differences between them are discussed. The chapter is concluded with a brief introduction of the tool used to generate C code for the real-time solvers used in both approaches.

3.1 Control structures

The energy optimization problem for the platoon is solved in two ways. A central approach and a decoupled approach, that is less computationally demanding, referred to as "greedy" method.

3.1.1 Centralized method

The problem defined in Section 2.5 can be solved in holistic manner where the platoon participants iteratively communicate their information to the cooperative controller which could be placed on either one of the vehicles or a cloud computer. The problem is then solved for the entire platoon and each of the vehicles receive back their respective optimal trajectories from the cooperative controller. In the centralized approach, participant vehicles cooperate to find a fuel-optimal solution for the platoon; a participant could compromise its own fuel saving if it results in a better fuel saving for the platoon.

The centralized method could also be thought of as a full knowledge strategy and it provides a fuel-efficient solution that is optimal for the entire platoon. This method is however computationally demanding since the complexity of the problem grows with the number of the vehicles in the platoon. Additionally, vehicles would be required to share more information in between them. Information to be shared include the masses, the engine limits, auxiliary power consumptions and frontal areas. The fact that more information sharing is required for the participants could raise some concerns as there might be a limit on the information that different manufacturers and freight transport companies are willing to share among them.

3.1.2 Greedy method

Since the holistic approach can prove computationally demanding and also because it requires the platoon participants to share more information between them, it would therefore be of interest to investigate a control strategy that can provide a sub-optimal solution compared to the centralized method.

In the greedy scheme, the optimization is solved backward per vehicle starting form the first vehicle. The first vehicle optimizes its fuel consumption based on the road information and communicates backwards what it has planned over the horizon. Subsequent vehicles base their optimal speed on both the road profile and the the speed profiles of the vehicles in front.

A limitation of this approach is that participants do not consider what is optimal for the platoon. The main advantages of the greedy method is that the computational demand does not increase with the number of vehicles in the platoon and vehicles needs not to communicate their masses, engine limits etc. The information that is communicated in the greedy method is limited to current positions and velocities and planned velocity profiles or time trajectories over the horizon.

Note that, if the platoon only consists of a single vehicle, there are no differences, whatsoever, between the centralized and the greedy method.

3.2 Variable change

To limit the number of linearizations required and also to obtain a purely convex problem, suitable variable changes can be adopted. This has been a popular method of removing non convex constituents of problems without the need for numerous approximations [8]. Note that linearizations will still be introduced even with a variable change but the number of elements to be approximated are tremendously reduced. In this thesis, as previously done in [8], the variable change of interest is to work with the kinetic energy which is a function of the squared velocity. As a side note, this particular approach of variable change i.e. transformation to the squared velocity has been used in optimal trajectory finding for robots [12].

For a certain vehicle occupying position i in the platoon, the kinetic energy is defined as

$$E_i(s) = \frac{m_{ei}}{2} v_i^2(s). \tag{3.1}$$

It then follows from (2.3) and (3.1) that

$$m_{ei}\frac{dv_i}{dt} = m_{ei}\frac{ds}{dt}\frac{dv_i}{ds} = m_{ei}v_i\frac{dv_i}{ds} = \frac{d}{ds}E_i \tag{3.2}$$

which states that the space derivative of the kinetic energy is equivalent to time derivative of the velocity. It can be easily verified that this variable change linearizes all the terms in (2.5) for a vehicle V_i with no surrounding cars, except for

the term related to auxiliary power consumption.

The nominal air resistance force exhibited in the absence of neighbouring vehicles can also be re-written as

$$F^0_{airi}(E_i) = \rho_a c_d A_f \frac{E_i(s)}{m_{ei}} \tag{3.3}$$

and the reduced air resistance force due to neighbouring vehicles becomes:

$$F_{airi}(E_i, d_{ji}) = \rho_a c_d A_f \frac{E_i(s)}{m_{ei}} \left(1 - \sum_j f_d(d_{ji}(s))\right). \tag{3.4}$$

Consequently, the state equation given in (2.5), can be re-written in terms of the energy as follow

$$\frac{d}{ds}E_i(s) = F_{Ei}(s) - F_{bi}(s) - F_{airi}(E_i(s)) - F_s(s) - \frac{P_{xi}}{f_{ti}(s)} \tag{3.5}$$

and the travel time dynamics given in (2.4) becomes

$$\frac{dt_i}{ds} = \frac{1}{v_i(s)} = f_{ti}(s) \tag{3.6}$$

where f_{ti} can be found, according to (3.1), as

$$f_{ti}(s) = \sqrt{\frac{m_{ei}}{2E_i(s)}}. \tag{3.7}$$

Note that it assumed that the vehicles do not stop or change course.

3.3 Discretization and platoon model

Given a sampling distance Δ_s, the two equations given in (3.5) and (3.6) can be written in the discrete domain as

$$E_i(k+1) = E_i(k) + \Delta_s \left(F_{Ei}(k) - F_{bi}(k) - F_{airi}(E_i(k)) - F_{si}(s) - P_{xi} f_{ti}(s)\right) \tag{3.8}$$
$$t_i(k+1) = t_i(k) + \Delta_s f_{ti}(s). \tag{3.9}$$

Note that (k) corresponds to discrete space instances over the planned horizon.

The reason for adopting spatial coordinates instead of time is due to the simple fact that hills are positioned at certain locations along the driving cycles. This makes it impossible to determine the hill location as a function of time unless the velocity profile of the vehicle is known beforehand. Using spatial coordinates allows for hill information to be modeled independently without the vehicle speed. This particular

discretization method has been adopted from the work being used as precursor for the thesis [8]; and was also used in two other master theses carried out by [13] and [14] where the authors mainly solved a closely related problem using the *MATLAB* software for disciplined convex programming also know as *CVX* [15].

The non-linear platoon model can be simply written as

$$E_i(k+1) = E_i(k) + \Delta_s\Big(F_{Ei}(k) - F_{bi}(k) - \\ - F_{airi}(E_i(k)) - F_{si}(s) - P_{xi}f_{ti}(s)\Big), \quad \forall i \in [1\ N] \tag{3.10}$$

$$t_i(k+1) = t_i(k) + \Delta_s f_{ti}(s), \quad \forall i \in [1\ N] \tag{3.11}$$

where N is the total number of the vehicles in the platoon.

3.4 Reference generation and energy limits

Clearly, the state equations given in (3.8)-(3.9) are nonlinear and require linearizarion around a reference trajectory of the kinetic energy.

Since the energy and the travel time dynamics, given in (3.8) and (3.9) respectively, are nonlinear in the kinetic energy E a reference kinetic energy, E_{ref}, is needed. The nonlinear terms in (3.8) and (3.9) can be linearized, before every iteration of the optimization, around the refrence E_{ref} .

As done in [8], a reference $v_{ri}(s)$ is computed for the vehicle V_i during every iteration based on a desired cruising speed $\bar{v}$, that can be set by the driver, the road velocity limits ($v_{\min}^{\text{road}}$, $v_{\max}^{\text{road}}$,) and the road profile along the prediction horizon. The assumption used is that the preferred cruising speed $\bar{v}\ \in [v_{\min}^{\text{road}}\ v_{\max}^{\text{road}}]$.

For a vehicle at position i in the platoon cruising at $v_{ri}(s)$, assuming no wheel slip, the maximum traction force, F_{Wmax}, that can be obtained at the wheels, at any gear γ, is found as

$$F_{Wmaxi}(\gamma, v_{ri}) = F_{Emaxi}(\gamma, v_{ri}) - F^0_{airi}(v_{ri}) - F_{si}(s) - P_{xi}/v_{ri}(s). \tag{3.12}$$

Given the maximum traction force F_{Wmax}, the reference velocity, $v_{ri}(s)$, can be obtained by solving the following numerical integration:

$$v_{ri}(s) = \min\left\{\bar{v}, \int_0^s \min\left\{\frac{a_{\max}}{v_{ri}(s)}, \max_{\gamma}\left\{\frac{F_{Wmaxi}(\gamma, v_{ri})}{m_{ei}v_{ri}(s)}\right\}\right\}ds\right\} \tag{3.13}$$

with an initial value $v_{ri}(0) = v_{i0}$, where v_{i0} is equivalent to the initial velocity of vehicle V_i that is read prior to the optimization. In (3.13), $a_{\max}$, in m/s^2, denotes the maximum permitted acceleration within a comfort zone. From the reference

velocity v_{ri} a reference kinetic energy E_{refi} can be easily obtained according to (3.1).

Linearizing around the reference speed v_{ri} implies that the actual optimal speed for the vehicle V_i does not significantly deviate from v_{ri}; as such the maximum and the minimum velocities are obtained by considering a maximum allowed deviation from the reference $\Delta v_{\max}$ and the road limits. The speed limits v_{mini} and v_{maxi}, for vehicle V_i, are found as

$$v_{\text{mini}}(s) = \max\left\{v_{\min}^{\text{road}},\ v_{ri}(s) - \Delta v_{\max}\right\}. \tag{3.14}$$

$$v_{\text{maxi}}(s) = \min\left\{v_{\max}^{\text{road}}, v_{ri}(s) + \Delta v_{\max}\right\}. \tag{3.15}$$

Similarly, as in the case for the reference kinetic energy, the maximum and the minimum kinetic energies, E_{mini} and E_{maxi} for vehicle V_i, are computed according to (3.1) from the maximum and the minimum velocities respectively. The maximum and the minimum kinetic energies are used as limits on their respective kinetic energies. More detail is found in Section 3.7.2

3.5 Gear selection and abstraction of the engine force

As done in [8], the gear selection is decoupled from the energy optimization; that is to say gear trajectory is known before the energy optimization. Although [8] used dynamic programing (DP) to optimize the gear, offline analysis showed that the fuel gain from optimizing the gear is small in contrast to the computation time. In the thesis, the gear at position k is set to the maximum that can maintain the reference velocity $v_{ri}(k)$ described in Section 3.4.

Since, the optimal velocity is allowed to deviate from the reference, the gear trajectory assumed at v_{ri} might not always be feasible. A traditional approach to counter this, is to include an abstracted model of the engine that can generate additional traction forces beyond its limits whenever a wrong gear is being used. This method was adopted from the work that is being used as precursor for the thesis [8]. The same method was previously presented in [16].

The engine transmission force,for a certain vehicle V_i in the platoon, is modelled as

$$F_{Ei}(s) = F_{E1i}(s) + F_{E2i}(s) \tag{3.16}$$

where $F_{E2i}(s)$ is only engaged when there is a need for a down shift; thus the usage of $F_{E2i}(s)$ will be associated with a cost, i.e. gear shift cost and is penalised accordingly in the cost function presented in Section 3.7.3.

Substituting the velocity with the kinetic energy using (3.1), and the torque with the engine traction force using (2.8) into the mass flow equation, shown in (2.7),

the mass flow per driven distance i.e. the fuel cost, $\tilde{\mu}_i(E_i, F_{Ei}) = \mu_i(\omega_i, T_{Ei})/v_i$, is found as

$$\tilde{\mu}_i(E_i, F_{Ei}) = a_0 f_t(E_i) + \sum_{j=1}^{2} \tilde{a}_j F_{E1i}^{j}(s) + \sum_{j=3}^{5} \tilde{a}_j E_i^{\frac{j-1}{2}}(s) + \tilde{a}_6 F_{E2i}(s) \tag{3.17}$$

where the new parameters are computed as

$$\tilde{a}_j = \begin{cases} \frac{a_j r^j(\gamma)}{\eta r(\gamma)} & \text{if } j = 1, 2. \\ \frac{a_j}{r^j(\gamma)(m_{ei}/2)^{\frac{j-1}{2}}} & \text{if } j = 3, 4, 5. \\ \frac{a_5}{\eta} & \text{if } j = 6. \end{cases} \tag{3.18}$$

The mass flow rate per travelled distance shown in (3.17) is used as a fuel cost and is penalized in the objective function of the control problem given in Section 3.7.3. Note that even though (3.17) is convex in all the optimization variables, only the linear and the quadratic terms are kept while the higher order terms are considered negligible. This simplification makes it possible to write to problem as quadratic program (QP).

3.6 Linearization and inter-vehicle distance approximation

The nonlinear terms in the kinetic energy and travel time equations, given respectively in (3.8) and (3.9), are the air drag force and the inverse velocity, f_t, referred to as *lethargy* in [8].

The function f_{ti}, corresponding to the lethargy of vehicle V_i, can be linearized around its respective reference kinetic energy E_{refi} as follow:

$$f_{ti}^{\text{lin}}(E_i) = f_{ti}(E_{refi}) + \left.\frac{\partial f_{ti}}{\partial E_i}\right|_{E_{refi}} (E_i - E_{refi}) \tag{3.19}$$

The term corresponding to the aerodynamic force in (3.8), also given in (3.4), is both non-convex and non-linear. Hence the aerodynamic force needs to be approximated to a linear and convex function that is suitable for computationally efficient quadratic programming.

If one denotes the inter-vehicle distance between vehicles V_i and V_j, that is found based on their respective reference velocities v_{ri} and v_{rj}, with $\hat{d}_{ji}$, then the air drag force can be approximated as

$$\begin{aligned} F_{airi}^{lin}(E_i, d_{ji}) =& \rho_a c_d A_f \frac{E_i(k)}{m_e} \left(1 - \sum_j f_d(\hat{d}_{ji}(k))\right) - \\ & - \rho_a c_d A_f \frac{E_{refi}(k)}{m_{ei}} \sum_j \left(d_{ji} - \hat{d}_{ji}\right) \left.\frac{\partial f_d}{\partial d_{ji}}\right|_{\hat{d}_{ji}} \end{aligned} \tag{3.20}$$

which is both linear and convex. Note that the index j can take up to two values as previously mentioned in Section 2.3.

The state equations of the kinetic energy and the travel time, given in (3.8) and (3.9), do not contain the inter-vehicle distance as a state and the definition of the inter-vehicle distance, given in (2.10), require the longitudinal positions of the vehicles to be known. Although it was mathematically shown in [8] that the longitudinal positions of all the platoon participants, with respect to the lead vehicle, can be found from the velocities, a reduced complexity formulation, where the longitudinal position were not required, was found to be more computationally efficient. In this thesis, the reduced complexity formulation,that is based on the assumption that the velocities do not deviate significantly from the cruising speed, $\bar{v}$, used in [8], is adopted.

Assuming the optimal speed of the vehicle V_i does not deviate significantly from $\bar{v}$, the distance between V_i and V_j can be estimated as

$$d_{ji}(s) = \bar{v}|t_j(s) - t_i(s)| - L_{ji}. \tag{3.21}$$

The absolute value can be disregarded since the order of the vehicles in the platoon is known prior to the optimization. Thus the distance between two vehicles simply becomes an affine, thus convex, function of the time headway in between them, i.e. the time, in seconds, it takes the vehicle in position j in the platoon to reach the vehicle in position i.

With the variable change introduced in Section 3.2, the abstracted engine model given in (3.16), and the bumper to bumper distance approximation given in (3.21), each of the platoon participants now have two states, t and E, and three control signals F_{E1}, F_{E2} and F_b. The optimizations variables for each of the vehicles include both its corresponding states and control signals.

3.7 The centralized approach

In the centralized method, the linear platoon model, presented in Section 3.7.1, is iteratively found by linearizing the nonlinear model, given in (3.10)-(3.11), around the reference kinetic energies. The gear trajectory is guessed based on the reference velocity, i.e. the maximum gear that can maintain the $v_{ri}(k)$ at position k is used for the vehicle V_i. The optimal kinetic energy are found by minimizing a convex quadratic performance index subject to the discrete state space model of the platoon and the limits on the optimization variables arising from the engine limits, road limits etc. The optimizer then outputs both the optimal state and input trajectories; in lieu of applying the optimal control input signals (forces) to the nonlinear platoon model, as traditionally done, the optimal state trajectories are supplied as references to existing lower layer controllers which generate suitable signals to the engine and brake subsystems.

3.7.1 Platoon model

It follows from Section 3.5 that there are five optimization variables at each MPC update for each of the vehicles in the platoon; that is two state variables and three control inputs. Namely the variables of interest are the kinetic energy $E(k)$, the travel time $t(k)$, the engine forces $F_{E1}(k)$ and $F_{E2}(k)$ and the braking force $F_b(k)$.

Since the inter-distance was approximated by the headway time between consecutive vehicles, the second vehicle has the travel time of the first vehicle in its equation of motion and subsequent vehicles have the travel time of the two leading vehicles in their equations of motion.

The state and input vector of a platoon of N vehicles, at a given position k can be written as

$$\mathbf{x}(k) = \begin{bmatrix} E_1(k) & t_1(k) & \dots & E_N(k) & t_N(k) \end{bmatrix} \tag{3.22}$$

$$\mathbf{u}(k) = \begin{bmatrix} F_{E11}(k) & F_{E21}(k) & F_{b1}(k) & \dots & F_{E1N}(k) & F_{E2N}(k) & F_{bN} \end{bmatrix}. \tag{3.23}$$

The platoon model can consequently be written as

$$\mathbf{x}(k+1) = \mathbf{A}(k)\mathbf{x}(k) + \mathbf{B}(k)\mathbf{u}(k) + \mathbf{W}(k), \quad k = 1, \dots H_p. \tag{3.24}$$

Note that in (3.24) the transition matrices $\mathbf{A}(k)$ and $\mathbf{B}(k)$ are space varying, i.e. not necessarily the same over the horizon, because the gear decision is carried out separately based on the reference velocities before the optimization and also because the road slope α changes from one position to another in the horizon. Before every iteration, gear trajectory is computed based on the reference velocity $v_{ri}(k)$; since higher gears are more efficient, the maximum gear, that is capable of maintaining the speed $v_{ri}(k)$ at position k, is selected. Selecting the gear based on the reference speed is evidently not as optimal as selecting it based on the optimal solution. But assuming the optimal speed does not deviate much from the reference, basing the gear on reference speed is still more favorable than enforcing a certain gear.

The term $\mathbf{W}(k)$ in (3.24) denotes known disturbances that arise from the rolling resistance force, the gravitational force and the linearizations. Just like the transitions matrices, the term $\mathbf{W}(k)$ is also space dependant.

3.7.2 Limits on the optimization variables

Under the assumption that the vehicles do not stop or change course, the velocity for a vehicle V_i is constrained to remain within the interval $[v_{\text{mini}},\ v_{\text{maxi}}] \quad \forall s \in [s_0,\ s_f]$ where s_0 and s_f indicate the start and the end of the horizon respectively; and v_{mini} and v_{maxi} are the speed limits computed according to (3.14)-(3.15).

The speed limit constraints are imposed in terms of the minimum and the maximum kinetic energies, previously presented in Section 3.4, as

$$E_{\text{mini}}(k) \leq E_i(k) \leq E_{\text{maxi}}(k), \quad \forall i \in [1 \;\; N]. \tag{3.25}$$

The travel time of each of the platoon participants is also upper-bounded by a maximum travel time. The maximum travel time for vehicle V_i is given by

$$t_{fi} = \int_{s_0}^{s_f} \frac{ds}{v_{ri}(s)}. \tag{3.26}$$

The upper bound on total travel times for the platoon participants is imposed as

$$t_i(s_f) \leq t_{fi}, \quad \forall i \in [1 \;\; N] \tag{3.27}$$

where $t_i(s_f)$ is time is takes vehicle V_i to reach the end of the horizon s_f. The constraint given in (3.27) can also be interpreted as a conservation of the average cruise speed in the sense that it imposes on the platoon participants to maintain $\bar{v}$ as the average speed over the horizon.

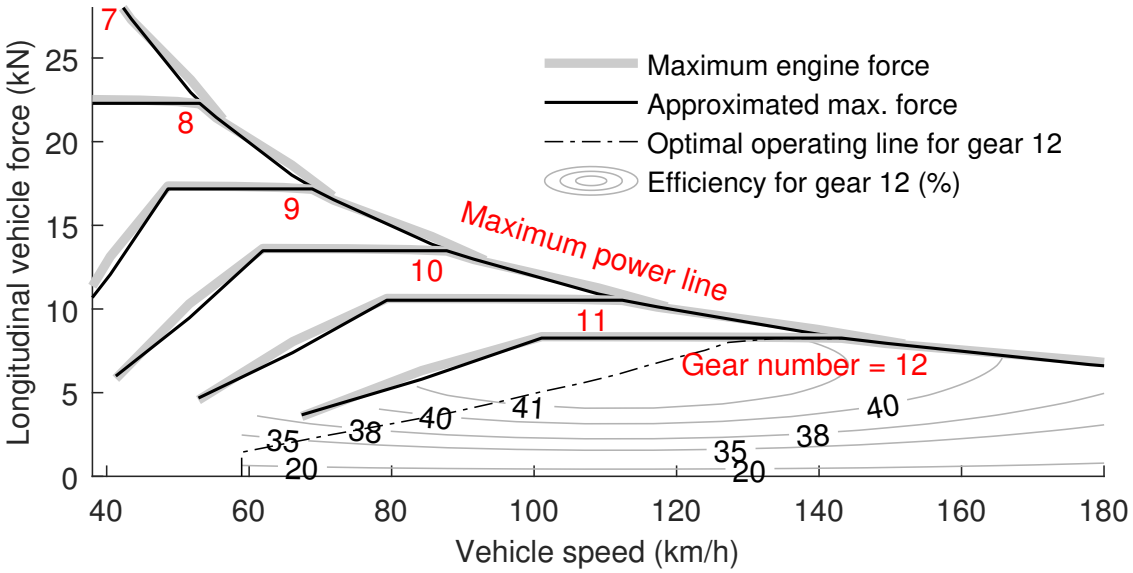

Figure 3.1: Maximum wheel force from the engine as a function of vehicle speed and gear.

The maximum longitudinal force at wheels side that the engine can provide, for each of the vehicle, varies with respect to the available engine torque, the selected gear and the vehicle speed as shown in Figure 3.1. The total engine forces, for a vehicle in position i in the platoon, is limited by the rated engine power P_{Emaxi} as

$$F_{Ei}(k) \leq \left(\frac{P_{\text{Emaxi}}}{v_i(k)} = P_{\text{Emaxi}} f_{ti} \right) \tag{3.28}$$

Substituting (3.16) and (3.19) into (3.28) gives the equivalent platoon constraint

$$F_{E1i}(k) + F_{E2i}(k) \leq P_{\text{Emaxi}} f_{ti}^{\text{lin}}(E_i) \leq \frac{P_{E\,\max}}{v_i(k)}, \quad \forall i \in [1 \;\; N] \tag{3.29}$$

which is an inner convex approximation of (3.28). $f_{ti}^{\text{lin}}(E_i)$ is the linearized lethargy presented in Section 3.6. More about convex-inner approximation can be found in [10].

The engine torque of vehicle V_i is also bounded between its corresponding idling torque and an approximated quadratic function of its velocity, resulting in the following constraints:

$$0 \leq T_{Ei}(k) \leq \min\{b_0, b_1 + b_2\omega_{Ei}^2(k)\}. \tag{3.30}$$

The constraint (3.30) can be equivalently written in terms of the optimization variables, i.e. the kinetic energy E_i and the engines force F_{E1i}, for the platoon as

$$\begin{cases} 0 \leq F_{E1i}(k)r(\gamma)/\eta \leq \min\{b_0, b_1 + \tilde{b}_2 E_i(k)\} \\ \tilde{b}_2 = b_2 \frac{2}{r^2(\gamma)m_{ei}} \end{cases} \Rightarrow$$
$$\Rightarrow \begin{cases} F_{E1i}(k) \geq 0 \\ F_{E1i}(k) \leq b_0 \\ F_{E1i}(k) \leq \tilde{b}_2 E_i(k) + b_1 \end{cases} \quad \forall i \in [1 \;\; N] \tag{3.31}$$

An additional constraint is that the force $F_{E2i}(k)$ and the braking force $F_{bi}(k)$ cannot be negative, i.e.

$$F_{E2i}(k) \geq 0; \; F_{bi}(k) \geq 0, \quad \forall i \in [1 \;\; N] \tag{3.32}$$

Furthermore, the vehicles in the platoon are constrained to maintain a minimum headway time from their respective lead vehicles; this is also equivalent to a minimum gap depending on the velocities. The safety requirement is imposed in terms of a minimum headway time as

$$t_i(k) - t_{i-1}(k) \geq t_{minh}, \qquad i = 2, \ldots, N \quad \forall k \in [s_0 \; s_f] \tag{3.33}$$

where s_f corresponds to the last sample of the horizon.

Since each of the platoon participants possesses their respective limits, i.e. the limits represented by (3.25)- (3.33), they can be easily transformed into a single compact constraint on both the sate and input vector of the platoon model; this can be written as

$$\mathbf{A}_{ineq}(k) \begin{bmatrix} \mathbf{x}(k) \\ \mathbf{u}(k) \end{bmatrix} \leq \mathbf{b}_{ineq}(k) \quad k = 1, \ldots H_p - 1 \tag{3.34}$$

$$\mathbf{A}_{ineq}(H_p)\mathbf{x}(H_p) \leq \mathbf{b}_{ineq}(H_p) \tag{3.35}$$

where H_p corresponds to the final sample of the prediction horizon.

3.7.3 Objective function

The objective function of the energy management problem of the platoon consists of two cost terms for each of the vehicles in the platoon. The most crucial cost term is the one related to the fuel cost. The different terms, penalized in the objective, include fuel cost and tracking error cost. The total cost to be minimized is the sum of each of these cost constituents for all the vehicles in the platoon. An additional penalty that could be considered is one that penalize the squared difference between consecutive forces, be they engine or braking forces; this can be seen as a jerk penalty. But since the predictive controller is intended to generate references for lower layer controllers, these controllers are assumed to be able to only allow comfortable jerks; as such drivability penalties are not considered.

For a vehicle occupying position i in the platoon, a simplified and quadratic fuel cost over the horizon can be found by discretizing and approximating (3.17) to a quadratic function in the states and inputs. The simplified and quadratic fuel cost adopted, for vehicle V_i, is found as

$$\begin{aligned} J_{\tilde{\mu}i} &= \Delta_s \sum_{k=1}^{H_p} \Big(a_0 f_{ti}(E_i) + \tilde{a}_1 F_{E1i}(k) + \tilde{a}_2 F_{E1i}^2(k) + \tilde{a}_3 E_i^2(k) + \tilde{a}_4 F_{E2i}(k) \Big) \\ &= \Delta_s \sum_{k=1}^{H_p} \left(\tilde{\mu}_i(k) \right) \end{aligned} \tag{3.36}$$

Since the first term of (3.36), weighted by a_0, represents the fuel cost when the engine is idling, it is equivalent to the penalizing the total travel time by a_0. Hence the fuel cost for vehicle V_i becomes

$$J_{\tilde{\mu}i} = a_0 \Big(t_i(N) - t_i(1) \Big) + \Delta_s \sum_{k=1}^{H_p} \Big(\tilde{a}_1 F_{E1i}(k) + \tilde{a}_2 F_{E1i}^2(k) + \tilde{a}_3 E_i^2(k) + \tilde{a}_4 F_{E2i}(k) \Big) \tag{3.37}$$

the equivalent total fuel cost for the platoon is then found as

$$J_{\tilde{\mu}T} = \sum_{i=1}^{N} J_{\tilde{\mu}i}. \tag{3.38}$$

The tracking cost is intended for when it is desired to track the reference kinetic energies that are discussed in Section 3.4. In such case, any deviation of the optimal energy from the reference energy, E_{refi}, for vehicle V_i, results in a cost weighted by w_{tr}; the tracking cost for a single vehicle V_i can be written as

$$J_{tri} = w_{tr} \sum_{k=1}^{H_p} (E_{refi}(k) - E_i(k))^2 = w_{tr} \sum_{k=1}^{H_p} \Big(e_{Ei}(k) \Big)^2 \tag{3.39}$$

where $e_{Ei}(k)$ denotes the deviation from the reference kinetic energy; and the equivalent tracking cost for the platoon is found as

$$J_{tr} = \sum_{i=1}^{N} J_{tri} \tag{3.40}$$

Note that for the tracking cost, the same weight w_{tr} is assumed for all the vehicles in the platoon; it is also assumed that each of the vehicles in the platoon have the same desired cruising speed.

The final objective function for the platoon, the sum of all the cost constituents, is found as

$$\mathbf{J} = J_{\tilde{\mu}T} + J_{tr} \tag{3.41}$$

The cost function, given in (3.41) can be rewritten as a sequential sum over the horizon, that is quadratic in $\mathbf{x}$ and $\mathbf{u}$, as follow

$$\begin{aligned}\mathbf{J} = \mathbf{x}^T(H_p)Q(H_p)\mathbf{x}(H_p) + f^T(H_p)\mathbf{x}(H_p) + \mathbf{C}(H_p) + \\ + \sum_{k=1}^{H_p-1} \left(\mathbf{x}^T(k)Q(k)\mathbf{x}(k) + \mathbf{u}^T(k)R(k)\mathbf{u}(k) + f^T(k)\mathbf{x}(k) + g^T(k)\mathbf{u} + \mathbf{C}(k)\right).\end{aligned} \tag{3.42}$$

Notice how the weight matrices are space dependant. This is related to the fact the fuel cost varies based on the selected gear according to (3.17). If one expands the constituent terms of the objective function, given in (3.41), there will be constant terms that are independent of the optimization variables which can be disregarded. Such terms are denoted by $\mathbf{C}(k)$ in (3.42)

3.7.4 The energy management problem

The energy optimization problem, i.e. the linear quadratic problem for the platoon is centered around the quadratic objective function given in (3.42), the discretized state space model of the platoon given in (3.24) and the linear inequality constraints on the state and input vector described by (3.34)-(3.35).

Given that the number of samples in the horizon is H_P, the optimization problem is formulated as

$$\min_{\mathbf{x},\mathbf{u}} \ \mathbf{J} \tag{3.43}$$

$$\begin{aligned} s.t \quad & \mathbf{x}(k+1) = \mathbf{A}(k)\mathbf{x}(k) + \mathbf{B}(k)\mathbf{u}(k) + \mathbf{W}(k), \quad k = 1 \dots H_p - 1 \\ & \mathbf{A}_{ineq}(k)\begin{bmatrix}\mathbf{x}(k)\\ \mathbf{u}(k)\end{bmatrix} \leq \mathbf{b}_{ineq}(k) \quad k = 1 \dots H_p - 1 \\ & \mathbf{A}_{ineq}(H_p)\mathbf{x}(H_p) \leq \mathbf{b}_{ineq}(H_p) \\ & \mathbf{x}(1) = \mathbf{x}_0 \text{ (fixed/known)}, \end{aligned}$$

Note that the problem defined in (3.43) could also be re-written into the standard form to be solved using *quadprog*. A brief description of the reformulation into the standard form is give in Appendix A.

3.8 The greedy approach

In the greedy method, the limits and the cost function for individual platoon participants remains the same. The inequalities, equalities and the bounds are decoupled and written for each of the vehicles individually. The minimum headway time constraints becomes only a bound on travel times of the following vehicles instead of a polytopic constraint on the travel times of consecutive vehicles in the platoon. The optimal kinetic energy are found by minimizing a convex quadratic performance index for a particular vehicle V_i subject to its respective discrete state space model and its limits. The optimizer then outputs both the optimal states and control input trajectories for that vehicle. Again the optimal state trajectory is supplied as references to the existing lower layer controller which then generate suitable input signals for the concerned vehicle.

The first vehicle in the platoon, V_1, will base its velocity profile on the topography information and the following vehicles will optimize their velocity profiles based on the topography information and on up to two of its predecessor's planned velocity profiles that it receives at every MPC update. This method assumes that each of the vehicles uses the same sampling distance and the same length of horizon.

The vehicle in the first position is fully decoupled from other vehicles, i.e. it does not need any information other than its own and the road profile to solve for its optimal speed. The following vehicles wait for up to two of the vehicles in front to send what they have planned over the horizon before they could solve for their respective optimal speed and gap profiles. The information received by following vehicles is treated as known disturbances. Note that this approach is not as fuel optimal as the centralized approach where there is cooperation between the platoon participants.

3.8.1 Individual vehicle model

If one denotes the state and the input vector of a vehicle occupying position i in the platoon at position k in the platoon with

$$x_i(k) = \begin{bmatrix} E_i(k) & t_i(k) \end{bmatrix}^T, u_i(k) = \begin{bmatrix} F_{E1i}(k) & F_{E1i}(k) & F_{bi}(k) \end{bmatrix}^T \tag{3.44}$$

then a state space model for an single vehicle, V_i,can be written as

$$x_i(k+1) = A_i(k)x_i(k) + B_i(k)u_i(k) + w_i(k). \tag{3.45}$$

just like in the case of the platoon, the transition matrices are space varying and same reasoning holds. $w_i(k)$ represents the known disturbances that arise from the

slope force and the linearization constants. Note that for vehicles other than the first vehicle, $w_i(k)$ also incorporates the received information from the preceding vehicles.

3.8.2 The energy management problem

The energy management problem is formulated for individual platoon participants as follow

$$\min_{x_i,u_i} \mathbf{J}_i = J_{\tilde{\mu}i} \tag{3.46}$$

$$\begin{aligned} s.t \quad & x_i(k+1) = A_i(k)x_i(k) + B_i(k)u_i(k) + w_i(k), \quad k = 1 \dots H_p - 1 \\ & A_{ineqi}(k) \begin{bmatrix} x_i(k) \\ u_i(k) \end{bmatrix} \leq b_{ineqi}(k) \quad k = 1 \dots H_p - 1 \\ & A_{ineqi}(H_p)x_i(H_p) \leq b_{ineqi}(H_p) \\ & x_i(1) = x_{i0} \text{ (fixed/known)}, \end{aligned}$$

Note that the minimum headway time constraint is now a simple bound on the travel times for vehicles other than the lead vehicle.

3.9 Code generation

Code generation for real-time solvers, that finds the optimal solutions to the energy management problem for the platoon in both the centralized and the greedy method, was one of aims of thesis. As such, FORCES Pro was used to generate real time MPC solver [17]. For code generation and implementation,a platoon consisting of three homogeneous vehicles is considered.
FORCES Pro requires the problem to be rewritten as multistage problem in the form

$$\min J = \sum_{k=1}^{N} \frac{1}{2} Z_k^T H_k Z_k + f_k^T Z_k \tag{3.47}$$

$$\begin{aligned} s.t \quad & D_1 Z_1 = c_1 \\ & C_{k-1} Z_{k-1} + D_k Z_k = c_k \\ & A_k Z_k \leq b_k \\ & \underline{z}_k \leq Z_k \leq \bar{z}_k \end{aligned}$$

where the Z_k vector contains all the optimization variables.

In the centralized approach, a single solver is generated whereas in the greedy approach two different solvers are required, one for the lead vehicle and a second for the

following vehicles. The reason for using two different solvers in the greedy approach is because the optimization problem of the first vehicle, in the greedy approach, is a less constrained problem compared to that of the following vehicles, i.e. it has no upper bounds on its travel time (except at $k = H_p$) since there is no vehicle in front of it. One could evidently opt to put very large bounds on its travel time so as the same solver can be triggered regardless of the vehicle's position in the platoon but a less constrained problem also means a faster computation time. Which also justify the need to have two different solvers in the greedy approach; and the appropriate solver could be triggered depending on the vehicle's position in the platoon.

With a fixed horizon length of 8 kilometer and a sampling distance of 80 meters, the code generated using FORCES pro for the centralized approach for a platoon formation of three vehicles requires about 3.3 million FLOPS per interior-point iteration for convergence; and the code generated for the greedy method requires only about 280 thousands FLOPS per interior-point iteration for each of the vehicles, i.e. less than a million FLOPS for the entire platoon. The number of FLOPS found for the two approaches suggest that the computation count in the greedy scheme is significantly reduced in comparison to the centralized approach.

4

Open loop solutions

This chapter presents the open loop solution for both a single vehicle and a platoon formation of three vehicles travelling on the test drive cycle at 80 km/h. The differences in the solutions found from the two approaches are presented together with the computation times on a standard portable computer. The base costs returned by the solvers, in each of the approaches, are used to estimate how much more fuel is consumed in the computationally efficient approach compared to the holistic approach.

In order to analyse the behaviour of the controllers and examine the computation times, it was deemed necessary to solve the problem for two horizon length using the first parts of the test driving cycle given in Section 2.4. This makes it possible to examine how much time it takes to solve the problem in both of the approaches. The minimum permissible update rates could be also determined based on the computation times. Note that although, kinetic energy is used as a state in the problem formulation, it is converted back to velocity after solving the problem according to

$$v_i = \sqrt{\frac{2E_i(k)}{m_{ei}}}; \tag{4.1}$$

also the weight for the tracking cost was set to zero in all the results presented in this chapter.

4.1 Optimal solution for a single vehicle

The optimal velocity profile for a single vehicle optimized with respect to the first two horizons of the test driving cycle is shown in Figure 4.1. The desired cruising speed was set to 80 km/h and the same is used as the initial velocity of the vehicle with a maximum allowed deviation of 5 km/h and a weight of 30×10^3kg. Other parameters used are found in Appendix B except for the ones deemed confidential.

As can be observed in Figure 4.1, the optimal velocity, marked by the solid blue line, remains within the velocity limits marked by the dashed magenta lines. The trend is that the vehicle slows down before uphill sections and speeds up at downhill sections as one would expect. The corresponding optimal force trajectories are also shown in Figure 4.1. Again the forces stay within the force limits and at very severe downhill locations the braking force is engaged; the brake is engaged at those locations to avoid going over the speed limits. Also the force F_{E2} was not engaged for this road

profile because the selected gear can handle the required force. If an infeasible gear was set before the optimization, the force F_{E2} would then be engaged and can be thought of as down shift.

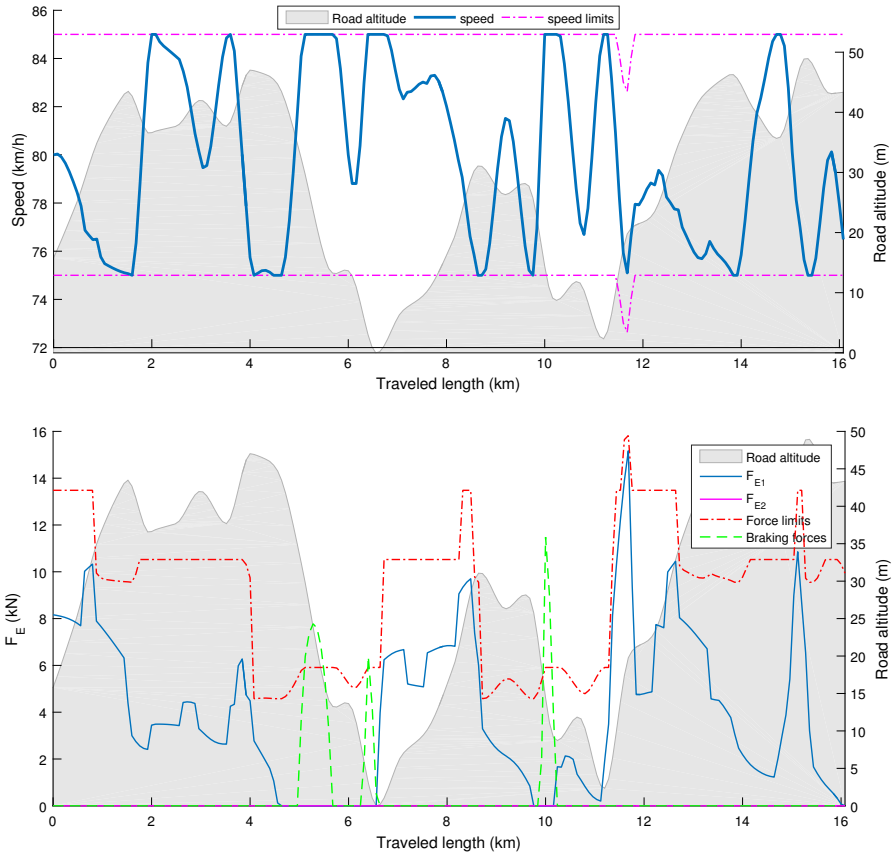

Figure 4.1: Optimal force and speed trajectories for a single vehicle of 30 tonnes with respect to the test driving cycle with 5 km/h allowed speed deviation (Top: Speed, bottom: Forces).

Allowing more deviations from the reference i.e. increasing the $\Delta v_{\max}$ would decrease the energy dissipated for braking; which is more fuel optimal. But this would in turn introduce linearization errors since the assumption that the optimal speed is always close to the reference no longer holds. The results of the simulation using $\Delta v_{\max} = 10$ km/h is depicted in Figure 4.2; it can be noticed in the figure that the peak of the braking forces are much lower compared to when a smaller deviation was allowed.

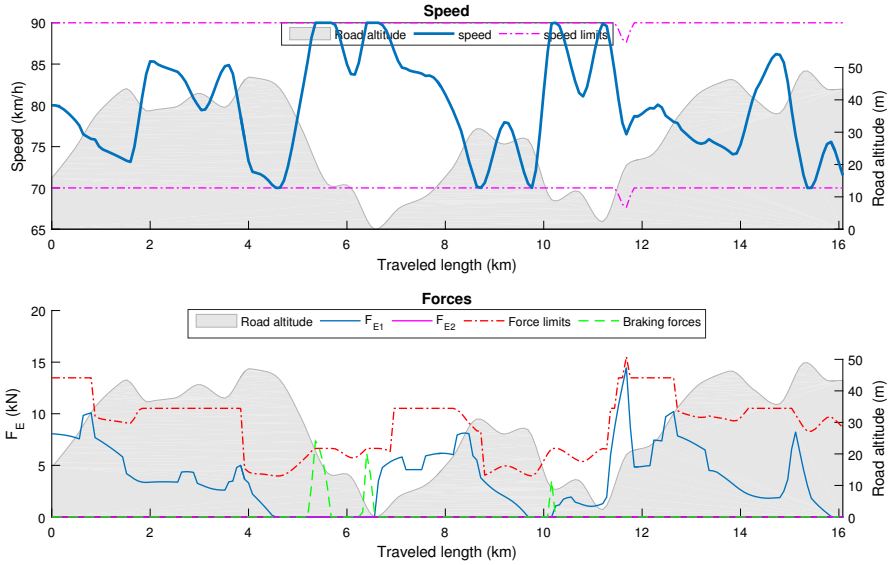

Figure 4.2: Optimal force and speed trajectories for a single vehicle of 30 tonnes with respect to the test driving cycle with 10 km/h allowed speed deviation.

.

4.2 Centralized approach

In order to examine the optimal solutions of the centralized approach for a platoon formation of three vehicles weighing 30 tonnes each, a cruising speed $\bar{v} = 80$ km/h was used and the initial velocity for each of the platoon participants was set to the cruising speed. The initial inter-vehicles distance is set to 20 meters that is a headway time of 0.9 seconds between the vehicles. The maximum allowed deviation from the speed reference was set $\Delta v_{\max} = 5$ km/h. With a minimum headway time of 0.8 seconds, the optimal velocity and headway time trajectories found are shown in Figure 4.3. For the speed trajectories, the blue, green and red solid lines represent the velocities for vehicles 1, 2 and 3 respectively; whereas in the gap trajectories, the blue solid line corresponds to the gap, in seconds, between vehicles 1 and 2 and the green solid line to the gap, in seconds, between vehicles 2 and 3.

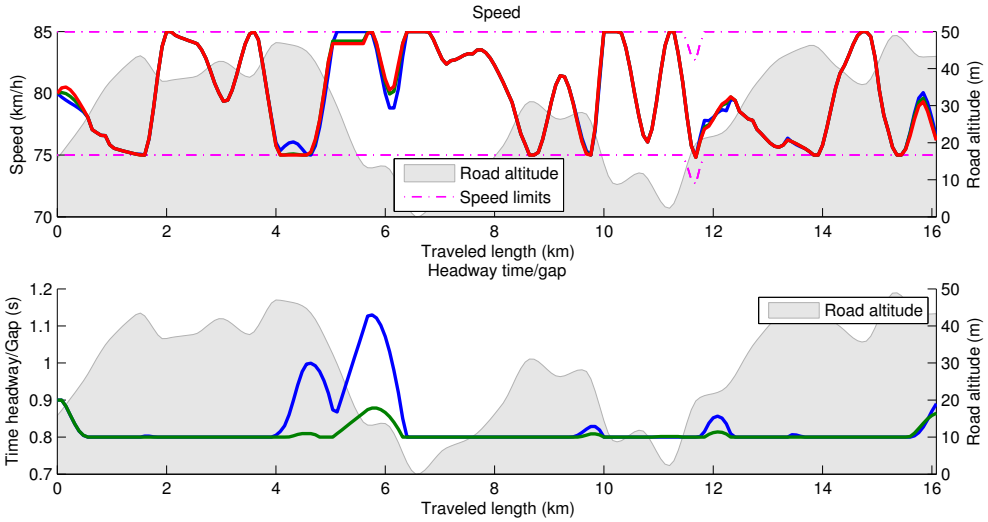

Figure 4.3: Optimal speed and gap trajectories for a platoon of three vehicles with respect to the test driving cycle with 5 km/h allowed speed deviation. For the speed trajectories, the blue, green and red solid lines represent the velocities for vehicles 1, 2 and 3 respectively; whereas in the gap trajectories, the blue solid line corresponds to the gap, in seconds, between vehicles 1 and 2 and the green the gap, in seconds, between vehicles 2 and 3.

As can be observed in Figure 4.3, the general trend is the same as in the case for a single vehicle i.e. the speed is decreased at the uphill segments and increased at the downhill segments resulting in the minimization of brake dissipation energy and the preservation of the average speed (80 km/h).

From the headway time of the last two following vehicles, it can be noticed that maintaining the minimum headway time, i.e. the shortest distance between the vehicles is optimal except at downhill segments where the lead vehicles increase their speed so that the respective following vehicles do not have to brake at those positions. One could intuitively say that vehicle one leaves the platoon temporarily at those locations.

The computation time is investigated on a standard PC (Intel i5- 2520M CPU at 2.5 GHz and 4 GB RAM). The computation time for a prediction horizon of 8 km and a sampling distance of 80 m is about 80 milliseconds which then dictates that the update rate in the closed loop MPC should be greater than 80 milliseconds.

4.3 Greedy approach

The optimal solutions for a three vehicle platoon, where each vehicle weights 30 tonnes, solved using the greedy approach, is depicted in Figure 4.4. The same settings were used as in solutions given Figure 4.3. The speed profiles is given in blue for the lead vehicle, in red for the second and in orange for the third vehicle. For the gap trajectories, blue represents the gap between the first two vehicles and green

represents the gap between the last two vehicles. The same trend is found in the velocity profiles as in the case for a single vehicle. The main difference is that, because there is no cooperation between the vehicles, the gaps at downhill sections are increased more than in the case of the centralized approach. This increase in the gap can be related to the fact that the lead vehicles no longer make compromises for the following vehicles and in turn the following vehicles avoid getting too close at down hills in order for them not to have to use the brakes. This increase in the gap at downhill sections results in an increase in the air drag losses, which in turns increases the fuel consumption of the platoon by a small percentage.

Comparing the base costs of the open loop solutions for the test drive cycle, the greedy approach increases the fuel consumption of the entire platoon by 1.5% for the test driving cycle for a homogeneous platoon of three vehicles weighting 30 tonnes each. Similar results were presented by [13] and [14]. Note that the difference in the fuel consumptions of the two approaches could evidently vary depending on the road profiles.

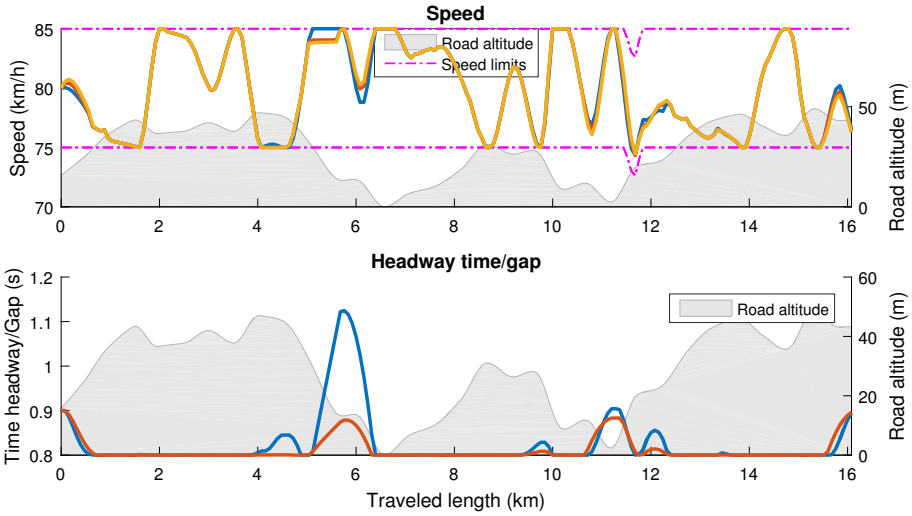

Figure 4.4: Optimal speed and gap trajectories for a platoon of three vehicles with respect to the test driving cycle with 5 km/h allowed speed deviation from 80 km/h (greedy method). The speed profiles is given in blue for the lead vehicle, in red for the second and in orange for the third vehicle. For the gap trajectories, blue represents the gap between the first two vehicles and green represents the gap between the last two vehicles

The computation time for a prediction horizon of 8 km and a sample distance of 80 meters on the same processor mentioned earlier is about 10 milliseconds per vehicle, resulting in an overall computation time of 30 milliseconds for the platoon. Clearly the computation time is tremendously reduced compared to the centralized approach. Note that, because the simulations were not performed on a dedicated computer, other running tasks could alter the computation times.

The conclusion from the open loop solution of test drive cycle, is that the greedy method reduces the computation time by about 63% at the expense of an 1.3% increase in the fuel cost for a platoon of three vehicles. With more vehicles in the platoon, the reduction in the computation time for the greedy approach could increase even further in comparison to the centralized method since the computation time in the latter increases exponentially with the number of platoon participants.

5

Closed loop simulations and fuel consumption analysis

In this chapter, the results found in the *Global simulation platform* (GSP) simulations, for the BLB drive cycle using the centralized method, are presented for both a single vehicle and a platoon formation of three homogeneous vehicles. In both cases, the fuel consumptions and the energy losses are compared to a model where a constant speed and gap are maintained over the entire road. Furthermore, comparative analysis between different masses, and update rates are carried out and the findings are presented.

5.1 Optimal solution for a single vehicle

This section presents the simulation results for a single 30 tonne vehicle. The velocity of the vehicle is planned with respect to the BLB road using the predictive controller. Note that for a single vehicle, no drag reduction is experienced.

The predictive controller is compared to a model where a constant speed is maintained by the vehicle over the route. Firstly, the simulation for the predictive cruise controller (PCC) was run for a specific distance and the trip time was recorded. In order to guarantee that the travel times are the same in both cases, the actual average speed maintained by the PPC is used as the cruising speed to be maintained by the truck with a fixed speed.

The predictive controller is planning for 8 km ahead with a sampling distance of 80 meters and a desired cruising speed of 75 km/h. The simulation results for the PCC and the fixed speed reference are shown in Figures 5.1 and 5.2. The PCC is triggered every 2 minutes.

In Figure 5.1 the trend is that the vehicle slows down on an uphill and speeds up on a downhill. At some positions where uphills are very steep the truck is driven with the lowest velocity due to its heavyweight and maximum power. Figure 5.2 shows how the local controller accurately tracks the constant speed reference. One can see that the controller is not following perfectly the reference speed which influences the comparison to some extent.

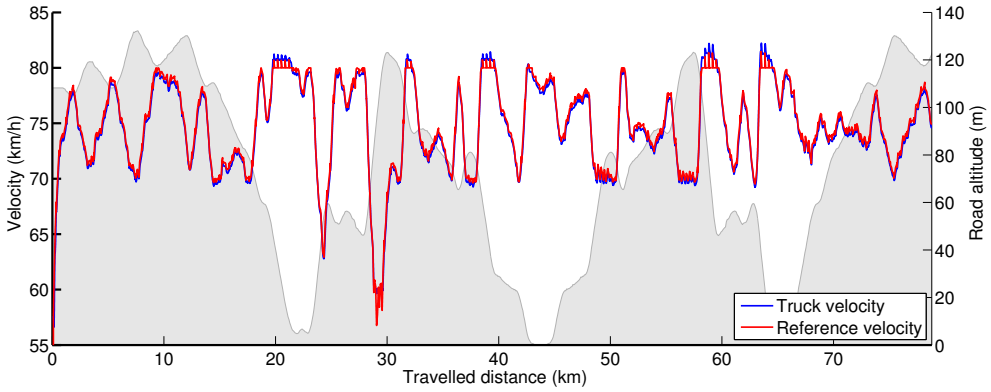

Figure 5.1: The velocity of a 30 tonnes truck on Borås-Landvetterusing-Borås road using the PCC updated every 15 seconds.

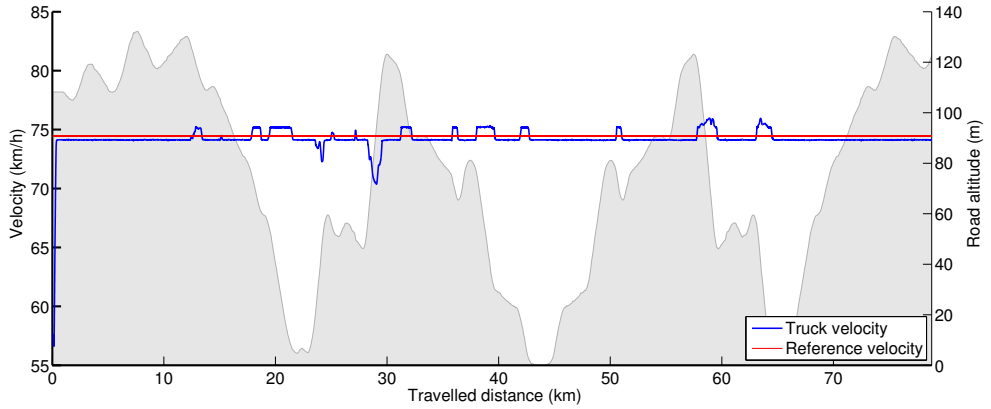

Figure 5.2: The velocity of a 30 tonnes truck on Borås-Landvetterusing-Borås road cruising at 74.47 km/h.

For a single vehicle, the fuel saving is related to both the speed profile and the energy dissipated in the brakes. Table 5.1 shows the fuel consumptions and the brake energy losses obtained from both the PCC and the fixed speed reference.

In table 5.1, it is noticeable that a truck cruising at a fixed velocity uses up more braking forces in order to maintain its constant velocity. Whereas in contrast, the predictive controller can speed up within the given tolerance to avoid this waste. The lethargies values show that the truck with an optimal velocity completes the driving cycle almost at the same time as the one with a fixed velocity. Regarding the fuel consumption, the predictive controller leads to 3.1 % improvement from the truck cruising at a constant speed.
Table 5.2 clarifies the effect of the update rates for PCC. It shows that the improvement from the fixed velocity cruise controller (FC) to PCC is bigger when a faster update rate is used. PCC gets more accurate data from the system by being triggered more frequently. Accordingly, the more accurate optimal reference is generated and sent to the local controller.

Table 5.1: Comparison between fixed velocity reference and optimal velocity reference.

Parameter	**Fixed velocity**	**Optimal velocity**	**Saving/loss%**
Fuel consumption (L/100km)	26.71	25.84	3.26
Brake energy loss (MJ/km)	4.09	3.93	3.76
Average lethargy (s/km)	48.50	48.40	0.21

Table 5.2: Fuel saving of the PCC compared to the FC with respect the update rate for a single vehicle.

	Update rate (PCC)		
	Every 15 seconds	Every 1 minutes	Every 5 minutes
Fuel saving with respect to FC (%)	3.26	3.19	3.04

5.2 Simulation results for a platoon formation of three vehicles

In order to evaluate how much fuel saving is achieved, closed loop simulations using the centralized approach were run using the nonlinear GSP models of Volvo AB. Before the closed loop simulations for the platoon, the minimum headway time safety constraints were relaxed by introducing slack variables. The purpose of the relaxation of the headway time constraint is to prevent possible infeasibilities that could occur whenever the lower layer controllers do not exactly follow the references provided by the predictive controller. Also, in the closed loop MPC, the predictive controller is run at slower rates compared to the lower layer controllers. After every MPC iteration, the optimal solutions over the 8 km horizon are stored before the next update and interpolation is used to find the references for the lower layer controllers based on the vehicles' current positions in the horizon.

Since the horizon starts from the position of the first vehicle, the following vehicles maintain their previous velocities or gaps after every update before they are in the current horizon. The simulations are carried out based on the *Borås-Landvetter-Borås* drive cycle using a maximum allowed deviation of 5 km/h from the speed reference and a minimum headway time of 0.8 seconds. The prediction horizon is set to 8 km with a sample distance of 80 meters.

The predictive cruise controller (PCC) is compared to a simple model where the lead vehicle cruises at a constant speed and the following vehicles maintain a constant headway time from their respective lead vehicles. This model will be referred to as "simple platoon controller" (SPC).

The constant cruising speed given to the SPC is always the actual average speed maintained by the PCC so that the travel times are the same in both the SPC and PCC simulations. Also in the SPC, the following vehicles always maintain the minimum headway time that is used as a minimum headway time in the PCC so that the drag reductions are in the same range.

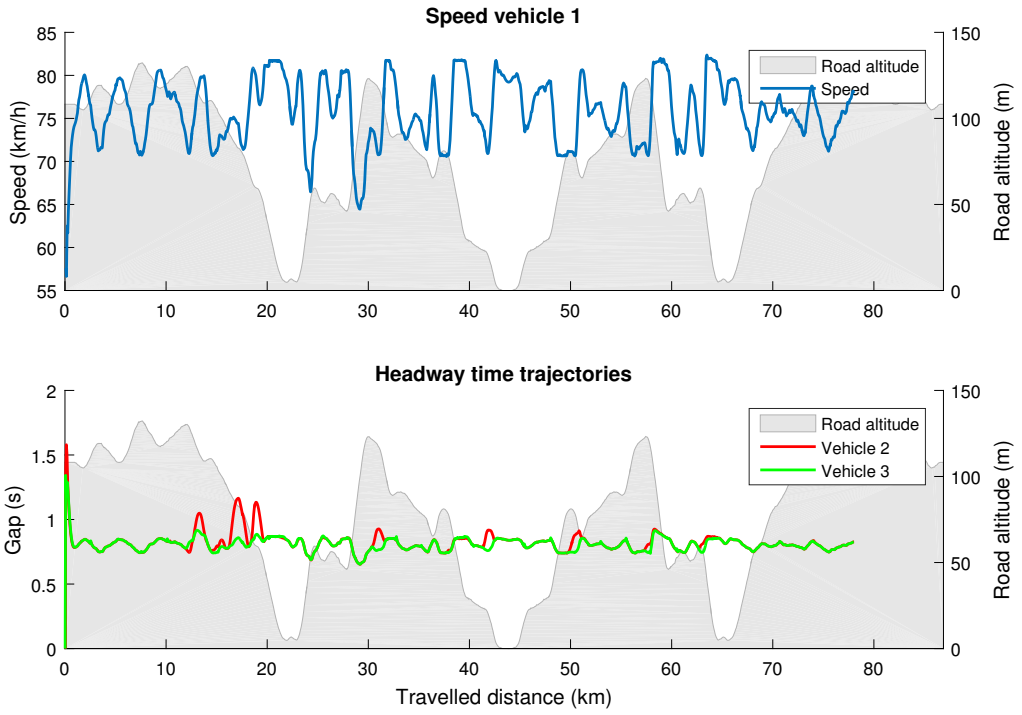

Figure 5.3: The velocity and inter-vehicle gap in seconds on the Borås-Landvetter-Borås road using the PCC updated every 2 minutes.

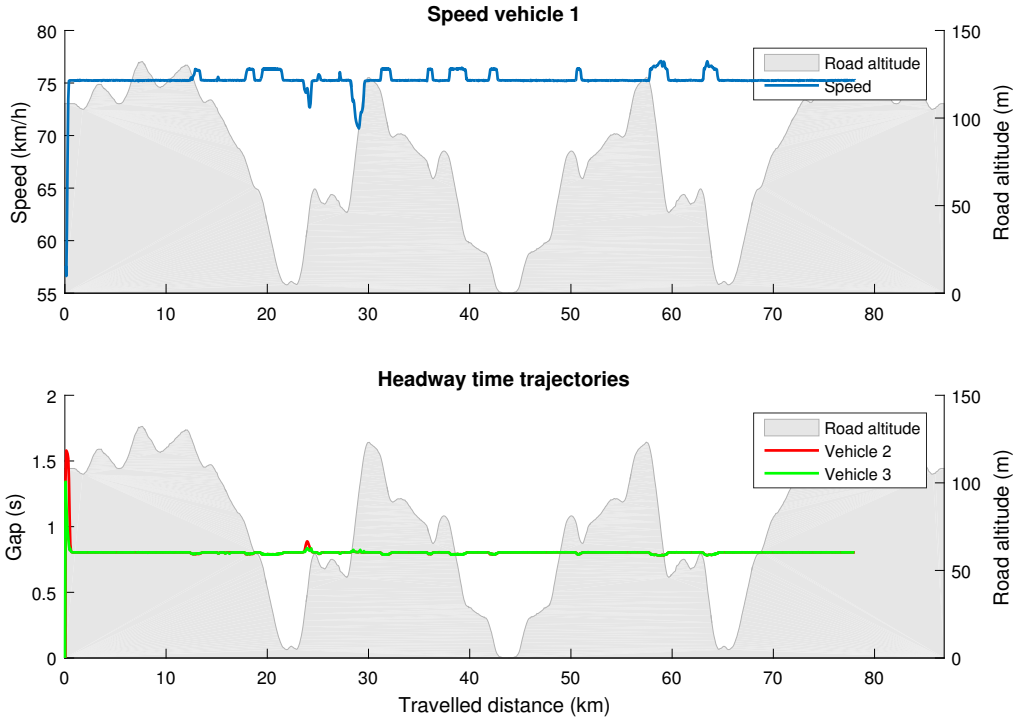

Figure 5.4: The velocity and inter-vehicle gap (in seconds) on the Borås-Landvetter-Borås road using the SPC.

The simulation results for a homogeneous platoon of three vehicles, weighting 30 tonnes each, obtained from the PCC, are shown in Figure 5.3 whereas the equivalent plot from the SPC is shown in Figure 5.4. The desired cruising speed was 75 km/h with 5 km/h allowed deviation. A minimum headway time of 0.8 seconds was used to maintain a minimum gap of about 16 meters.

A similar behaviour is noticed in the speed trajectories, found using the PCC, as in the open loop simulations; the speed of the lead vehicle is increased at downhill sections and decreased at uphill sections. The headway time is kept at the minimum except at the noticeable downhill sections where it is increased to prevent the following vehicles from using the brakes.

It can also be seen in Figure 5.3 that the speed drops as low as 65 km/h at very steep uphill locations due to the vehicles' weight and the maximum power limits. The drop in the speed trajectory does not introduce infeasibilties because a new reference is generated iteratively during every MPC update based on road section as discussed earlier in Section 3.4. And the new speed limits are always formed around the reference. Note that the road limits are not activated here.

Similar drops in the speed trajectory are noticed at very steep uphill locations even in the case of the SPC depicted in Figure 5.4. It can additionally be noticed that the lower layer controllers do not follow the supplied reference trajectories at very severe down hill sections, where the vehicles gain energy from gravity and the controller

responds by braking but not quickly enough to result in an error-free tracking of the provided references.

Table 5.3 shows the fuel consumptions and the energies per kilometer for the PCC and the SPC. Also given in Table 5.3, are the fuel savings for each of the platoon participants and overall saving for the platoon as well as the average travel times per kilometer (lethargy) of both the PCC and the SPC.

Table 5.3: Fuel consumption and energies from the SPC and PCC for a homogeneous platoon of 3 vehicles weighing 30 tonnes cruising at 75 km/h on the *Borås-Landvetter-Borås* drive cycle.

	SPC				**PCC**				**Saving/loss (%)**			
	V1	V2	V3	Platoon	V1	V2	V3	Platoon	V1	V2	V3	Platoon
Fuel consumption [L/100km]	26.93	25.27	24.88	77.08	25.84	24.15	23.68	73.67	4.24	4.61	5.04	4.62
Air drag loss [MJ/km]	1.66	1.28	1.17	4.07	1.69	1.3	1.19	4.14	-1.43	-1.58	-1.61	-1.53
Brake energy loss [KJ/km]	4.12	3.84	3.77	11.72	3.96	3.65	3.57	11.20	3.91	4.98	5.33	4.71
Average lethargy [s/km]	-	-	-	47.77				47.59	-	-	-	0.37

From the data in Table 5.3, it can be deduced that the PCC results in a more fuel optimal driving compared to SPC; individually for each of the platoon participants and the overall platoon. In the SPC, the lead vehicle would only maintain a constant speed; which requires frequent usage of the brakes specially at downhill sections. As a results the following vehicles, constantly trying to maintain a constant headway time, engage the brakes even more often. The PCC, on the other hand, works towards preventing the usage of brakes as much as possible for all the platoon participants by allowing the vehicles to speed up at downhill segments and slow down at uphill segments. As seen in the open loop solution in Chapter 4, the PCC increases the gap at downhill sections to prevent the direct usage of the brakes. The increase in gap also results in air drag energy losses. The retarding forces from the drag losses are used for moderate braking at downhill segments. This phenomenon can also be verified by comparing the braking and the air drag forces over the drive cycle.

A plot of the air drag forces and braking forces for the SPC and the PCC are shown in Appendix C, Figure C.1 and Figure C.2 respectively; the plots show that the brakes are used more frequently in the SPC compared to PCC. The PCC increases the retarding forces from the air drag; thus vehicles do not have to engage in braking except at very severe downhill sections where the brakes are engaged to adhere to the average velocity constraint that is imposed on each of the platoon participants.

Table 5.3 Shows a fuel saving of 4.41% for the three-vehicle platoon travelling on the *Borås-Landvetter-Borås* drive cycle when the PCC is used instead of the SPC and the total travel time per kilometer, denoted by lethargy in Table 5.3, is also smaller in the PCC. So the PCC does not only finish the journey faster but also with better fuel saving. Notice how the lethargy reflect the 75 km/h average speed over drive cycle. The SPC takes slightly more time per kilometer because of the drop in the speed at uphill sections which it is not able to make up for at downhill sections.

The fuel saving of the PCC is mainly due the lessened usage of the brakes. But the minimization of the braking energies is done at expense of the air drag losses for each of the platoon participants especially for the last vehicles since its drag reduction contribution is from both of the two leading vehicles. The last vehicle also saves the most on braking because both the two lead vehicles' speed are planned so that it does not require braking at downhill segments.

At a first glance to Tables 5.1 and 5.3, one might question why the amount of fuel consumed for a single vehicle cruising at constant speed with no drag reduction, given in Table 5.1, is lesser than the one of the lead vehicle (V1) with drag reduction i.e. the SPC case given in Table 5.3. But the reason for that is that the simulations were done using different cruising speeds. In fact, the one given in Table 5.3, finishes the journey earlier i.e. it is cruising at a higher speed. This is also reflected by the lethargies per kilometer provided in the respective tables. If in fact the two simulations were done using the same fixed reference, the lead vehicle would consume less in the platoon than when it is alone with no neighboring vehicles.

The above results were all found by triggering the PCC every two minutes; with a prediction horizon of 8 km and an average cruising speed of 75 km/h. This update rate of the PCC is enough for consecutive MPC updates to overlap. That is to say the vehicles will not travel more than the 8 km horizon in two minutes while maintaining the average speed. Triggering the PCC more often is indeed more beneficial for the case of a single vehicle since it will always be within the horizon and it will always receive an optimal reference from the PCC . However, for a platoon, the following vehicles (2 and 3) will always be outside the horizon every time the PCC is triggered; and they are made to maintain their current speed until they are in the new horizon which might no longer be the optimal speed at those positions. Consequently updating very frequently introduces errors for the following vehicles and is thus not beneficial in that sense. A workaround to this could be to always store the optimal solutions for 2 consecutive updates and allow the following vehicles to base their references on one of these solutions depending on their positions. This is however not investigated further in this thesis.

Likewise, not updating very often could also introduce errors, be it a platoon or a single vehicle, simply because the lower layer controllers do not follow the references exactly. The optimum update rate for an average cruising speed of 75 km/h was found, based on test runs, to be 2 minutes. Table 5.4 shows the fuel consumptions

for the platoon with the same settings as for the results given in Table 5.3 with different update rate for the PCC. The 2 minutes update rate resulted in the best fuel saving for a cruising speed of 75 km/h on the BLB road profile.

Table 5.4: Fuel saving of the PCC compared to the SPC as a function of the update rate of the PCC.

	Update rate (PCC)		
	Every 1 minute	Every 2 minutes	Every 4 minutes
Fuel saving with respect to SPC (%)	4.36	4.62	4.42

The simulation results for the same platoon formation and the same settings with the exception that the weights are set to maximum, i.e. 44 tonnes, are shown in Figures 5.5 and 5.6. The same behaviour, as in the case when 30 tonnes vehicles were used, is observed. The main difference is that, due to the heavy load, it is now hard to maintain the average speed over the drive cycle for both the SPC and the PCC due to the drop in the speed at noticeable uphill sections. But the deviation from the average speed is worse in the SPC compared to the PCC since the later can make up for the delays at downhill sections where it lets the platoon speed up. This also suggest that, instead of having a fixed desired cruising speed $\bar{v}$ for the platoon, a space dependent one could be more preferable where lower cruising speed could be imposed in sections with very steep hills. This can be thought of as relaxation of the constraint that dictates the conservation of the average speed.

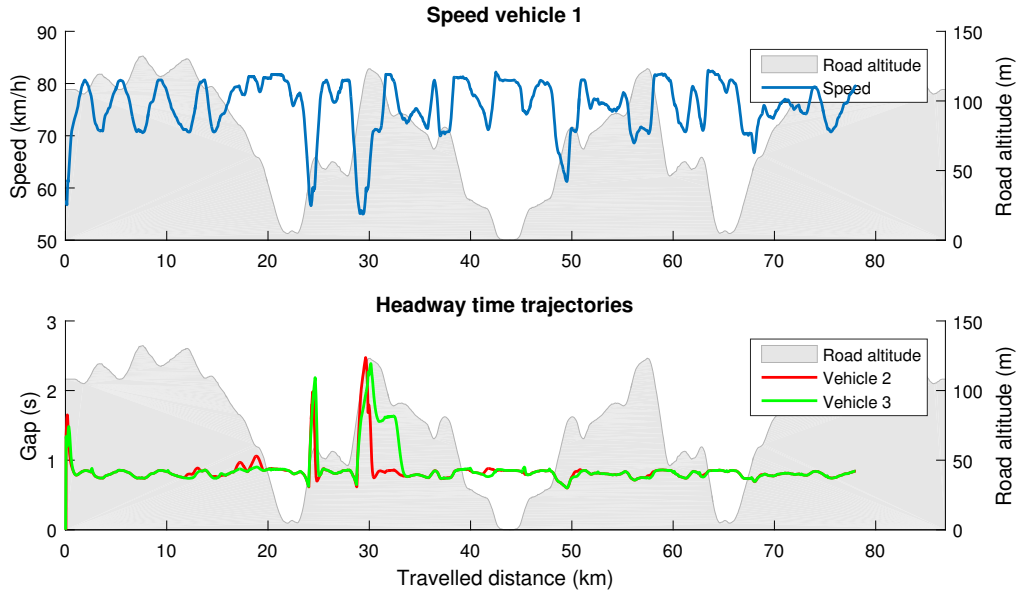

Figure 5.5: Speed and inter vehicle gap profiles for a platoon of 3 vehicles travelling on the Borås-Landvetterusing-Borås road using the PCC updated every 2 minutes (44 tonnes each).

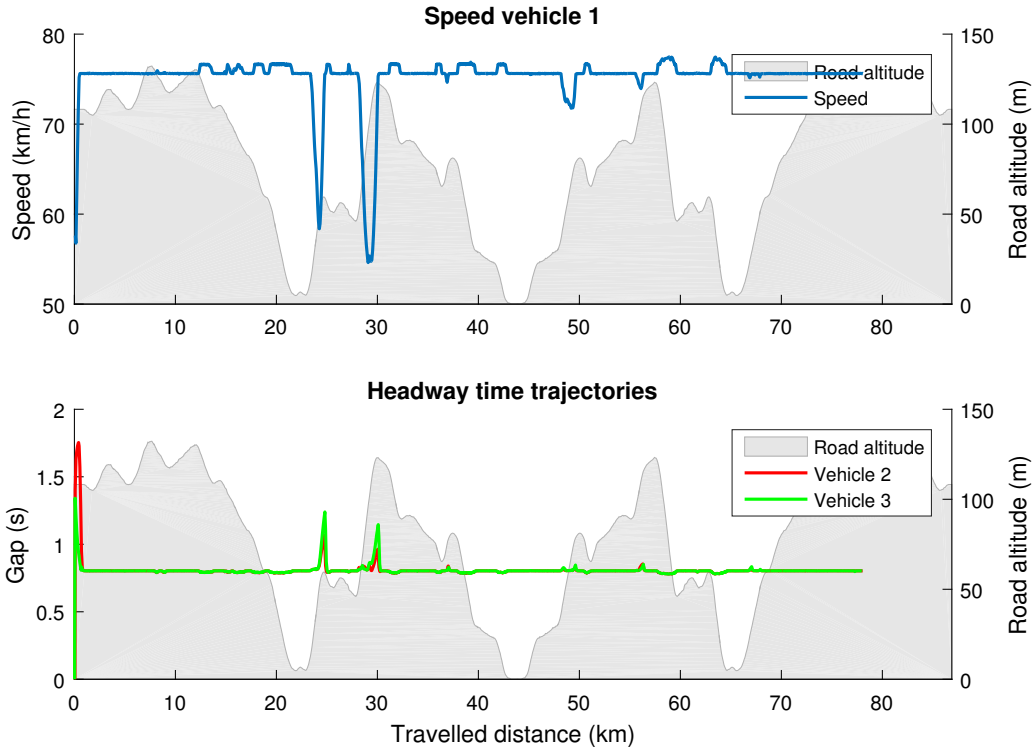

Figure 5.6: Speed and inter vehicle gap (in seconds) on the Borås-Landvetterusing-Borås road using the SPC for a platoon of three vehicles of 44 tonnes each.

Since the various energies are directly proportional to the vehicles weights; a notice-

able increase in the fuel saving percentage is obtained. Table 5.5 shows the various energy losses and the amount of fuel consumed for the platoon using the SPC and the PCC for vehicles weighting 44 tonnes.

Table 5.5: Fuel consumption and energies from the SPC and PCC for a homogeneous platoon of 3 vehicles weighing 44 tonnes and cruising at 75 km/h on the *Borås-Landvetter-Borås* drive cycle

Parameters	**SPC**	**PCC**	**Saving/Loss (%)**
Fuel consumption [L/100km]	99.98	94.68	5.592
Air drag energy losses [MJ/km]	4.115	4.1724	-1.375
Brake energy losses [kJ/km]	15.588	14.724	5.871
Average lethargy [s/km]	47.9302	47.8919	0.0799

Although the energies for individual vehicles are not shown in Table 5.5, they follow the same trend as in Table 5.3. That is to say, the majority of the overall fuel saving contribution for the platoon comes from the vehicles occupying the end of the platoon. For the BLB road profile, a fuel saving of about 5.6% is achieved for a platoon of 3 identical vehicles weighting 44 tonnes each.

The fuel saving is expected to increase even further for road profiles that are more hilly; also it has been seen that the lower layer controllers do not exactly follow the reference trajectories provided; having local controllers that are more aggressive, the SPC would use the brakes even more frequently whereas the PCC would prevent even more the usage of the brakes; which in turns would increase the amount of fuel saved per kilometer.

From the open loop simulations, it was found from the base costs that the greedy approach will reduce the computation time by 63% while increasing the fuel cost by 1.3%, the same results is expected to hold for the closed solutions although actual closed loop simulations, using the greedy method, are required to confirm these figures.

6
Conclusion

The thesis presented two types of predictive cruise controllers that, in a moving horizon approach, plan the speed and the inter-vehicle distance for heady duty vehicles driving in a hilly terrain. Real-time solvers were generated for both controllers using FORCES Pro.

The centralized cooperative cruise controller, proposed in this thesis, optimizes the fuel consumption for the platoon and it requires sharing of private information between the platoon participants. The second method proposed, is a greedy approach where there is no cooperation between the vehicles forming the platoon, i.e. private information need not be shared among the vehicles.

Open loops solutions for a test road profile show that the greedy method is computationally efficient compared to the centralized method although the latter results in about 1.3% fuel saving with respect to the former. Similar results are expected to hold for the closed loop case but actual MPC simulations in GPS are required for validation.

Closed loop MPC simulations in GSP, using the predictive controller, showed that a fuel economy improvement of up to 3.26% is achieved for single vehicle driving on the BLB road. The GSP simulations also showed that up to 5.6% of fuel saving is achieved by the cooperative PCC, for a homogeneous three vehicle platoon travelling on the BLB road, compared to the SPC. The PCC did not only improve fuel saving, but also shortened the travel time of the platoon.

7
Future Work

The current control strategies are based on linearizations around speed references and assume that the optimal speeds remain close to the references. This introduces linearization errors specially for higher speed tolerances. Hence implementing the Newton direction cost, proposed and used in [8], to remove linearization errors could improve the current algorithm.

The gear trajectory is based on reference speeds and is not optimized. For very hilly roads with severe uphill sections, given that consecutive MPC updates overlap, it might be more favorable to base the gear trajectories on the most recent optimal speeds and incorporate, for instance, the dynamic programing algorithm proposed by [8], into the current strategies.

The results found are based on homogeneous platoon formations. It is thus interesting to investigate scenarios where the platoon is comprised of vehicles with different characteristic; such as masses, maximum engine power, etc. In such scenarios, changes are needed in the current strategies to avoid infeasibilties. For instance the average cruising speed needs to be maintainable by all platoon participants. Also in such scenarios, the ordering of the vehicles, depending on their power limits and frontal areas, could play a major role in the fuel consumption of the platoon.

The current strategy uses interpolation to decide the reference speed or gap for the platoon participants depending on their respective positions in the horizon. Given that the horizon starts from the lead vehicle's position, the following vehicles are always outside the horizon after every update; they are thus made to maintain their previous speed or headway times until they are in the current horizon. An imperative feature to add to the current strategy would be to store the two most recent optimal solutions so the lower layer controller of the following vehicles always listen to an optimal solution in lieu of maintaining their respective previous references, which might no longer be optimal, before they are in the current horizon.

Furthermore, additional simulations in GSP are needed to analyze the impact of shorter sampling distances, different drive cycles and possibly longer horizon lengths.

Bibliography

[1] L. Bühler. "Fuel-efficient platooning of heavy duty vehicles through road topography preview information". MA thesis. Stockholm, Sweden: KTH, 2013.

[2] A. Alam. "Fuel-efficient heavy-duty vehicle platooning". PhD thesis. Stockholm, Sweden: KTH, 2014.

[3] A. Alam et al. "Heavy-duty vehicle platooning for sustainable freight transportation: A cooperative method to enhance safety and efficiency". In: *IEEE Control Systems Magazine 35* (June 2015), pp. 34–56.

[4] E. Hellström et al. "Look-ahead control for heavy trucks to minimize trip time and fuel consumption". In: *Control Engineering Practice 17* (Feb. 2009), pp. 245–254.

[5] L. Nielsen E. Hellström J. Åslund. "Design of an efficient algorithm for fuel-optimal look-ahead control". In: *Control Engineering Practice 18* (Nov. 2010), pp. 1318–1327.

[6] R. Bellman. *Dynamic Programming and Optimal Control*. New Jersey: Princeton Univ Pr, 1957.

[7] Bo Egardt. *Model Predictive Control*. Lecture Notes. 2015.

[8] N. Murgovski, B. Egardt, and M. Nilsson. *Cooperative energy management of automated vehicles*. Submitted to Control Engineering Practice. 2016.

[9] Olof Lindgärde et al. "Optimal Vehicle Control for Fuel Efficiency". In: *SAE International Journal of Commercial Vehicles* (2015), pp. 682–694.

[10] Stephen Boyd. *Convex Optimization*. Cambridge University Press, 2004.

[11] V. Turri et al. "Fuel-efficient heavy-duty vehicle platooning by look-ahead control," in: *53rd IEEE Conference on Decision and Control,* 2014, pp. 654–660.

[12] T Lipp and S Boyd. *Minimum time speed optimization along a fixed path*. International Journal of Control 87 (6). 2014.

[13] Mandus Jeber. *Fuel efficient control of vehicle platoons using road topography information*. Master thesis. 2015.

[14] John Wahnström. *Energy Optimization for Platooning through Utilizing the Road Topography*. Master thesis. 2015.

[15] Michael Grant and Stephen Boyd. *CVX: Matlab Software for Disciplined Convex Programming, version 2.1*. `http://cvxr.com/cvx`. Mar. 2014.

[16] L. Johannesson et al. "Predictive energy management of hybrid long-haul trucks". In: *Control Engineering Practice 41*. 2015, pp. 89–97.

[17] Alexander Domahidi and Juan Jerez. *FORCES Professional*. embotech GmbH (`http://embotech.com/FORCES-Pro`). July 2014.

A

Formulation into standard quadratic form

The optimization problem given in (3.43) can to be reformulated into the standard quadratic form for it to be solved using *quadprog* and other solvers. The equality and inequality constrained standard problem is written in standard form as

$$\min_{\mathbf{z}} \; f(\mathbf{z}) = \frac{1}{2}\mathbf{z}^T\mathbf{H}\mathbf{z} + \mathbf{g}^T\mathbf{z} \tag{A.1}$$
$$s.t \qquad \begin{cases} C\mathbf{z} = b_{eq} \\ \mathbf{A}\mathbf{z} \leq b \end{cases}$$

The optimization variables over the horizon are all included in the $\mathbf{z}$ vector and can be set as

$$\mathbf{z} = [\, \mathbf{x}^T(1) \quad \mathbf{u}^T(1) \quad \dots \quad \mathbf{x}^T(H_p-1) \quad \mathbf{u}^T(H_p-1) \quad \mathbf{x}^T(H_p) \,]^T. \tag{A.2}$$

With the above choice of the optimization vector and referring back to (3.42) one can easily construct the extended weighting matrix over the horizon $\mathbf{H}$, also known as the Hessian from, as follow

$$\mathbf{H} = 2 \begin{bmatrix} Q(1) & & & & & & \\ & R(1) & & & & & \\ & & \ddots & & & & \\ & & & Q(H_p-1) & & & \\ & & & & R(H_p-1) & & \\ & & & & & Q(H_p) \end{bmatrix}, \tag{A.3}$$

Similarly, the weighting penalty of the linear terms $\mathbf{g}$ of (A.1) is constructed as

$$\mathbf{f} = \begin{bmatrix} f^T(1) & g^T(1) & \dots & f^T(H_p-1) & g^T(H_p-1) & f^T(H_p) \end{bmatrix}^T \tag{A.4}$$

Additionally, by expanding (3.24) over the prediction horizon H_p one obtains the equality constraint $C\mathbf{z} = b_{eq}$ with the following matrices:

$$C = \begin{bmatrix} \mathbf{A}(1) & \mathbf{B}(1) & -I & & & & \\ & & \mathbf{A}(2) & \mathbf{B}(2) & -I & & \\ & & & \ddots & & & \\ & & & & & A(H_p-1) & B(H_p-1) & -I \end{bmatrix}, b_{eq} = - \begin{bmatrix} \mathbf{W}(1) \\ \mathbf{W}(2) \\ \vdots \\ \mathbf{W}(H_p-1) \end{bmatrix} \tag{A.5}$$

Furthermore the inequality constraint matrices $\mathbf{A}$ and $\mathbf{b}$ of (A.1) can be easily found by again expanding (3.34)-(3.35) over the horizon. The $\mathbf{A}$ and $\mathbf{b}$ matrices are found as

$$\mathbf{A} = \begin{bmatrix} \mathbf{A}_{ineq}(1) & & & & \\ & \mathbf{A}_{ineq}(2) & & & \\ & & \ddots & & \\ & & & \mathbf{A}_{ineq}(H_p-1) & \\ & & & & \mathbf{A}_{ineq}(H_p) \end{bmatrix}, \; b = \begin{bmatrix} \mathbf{b}_{ineq}(1) \\ \mathbf{b}_{ineq}(2) \\ \vdots \\ \mathbf{b}_{ineq}(H_p) \end{bmatrix} \tag{A.6}$$

B

Model Parameters

Table B.1: Model parameters

Parameter	**Notation**	**Value**	**Unit**
Total vehicle mass	m	(30,44)	tonne
Aerodynamic drag coefficient	c_d	0.6	m^2
Air density	ρ_a	1.3404	kg/m^3
Gravitational acceleration	g	9.81	m/s^2
Engine maximum power	P_{Emax}	330000	W
Auxiliary power	P_{aux}	3000	W
Highest gear	γ_{max}	12	-
Frontal area	A_f	8.75	m^2

C

Air drag and braking forces on BLB drive cycle from SPC and PCC

Plots of the forces from the GSP simulation of homogeneous platoon of three vehicles weighting 30 tonnes and cruising at 75km/h with a maximum allowed deviation of 5km/h and minimum time headway of 0.8 seconds. The color order is blue for the lead vehicle, red for the second vehicle and orange for the third vehicle. Notice that the braking forces the first and the second vehicle are smaller compared to the third vehicle in both cases.

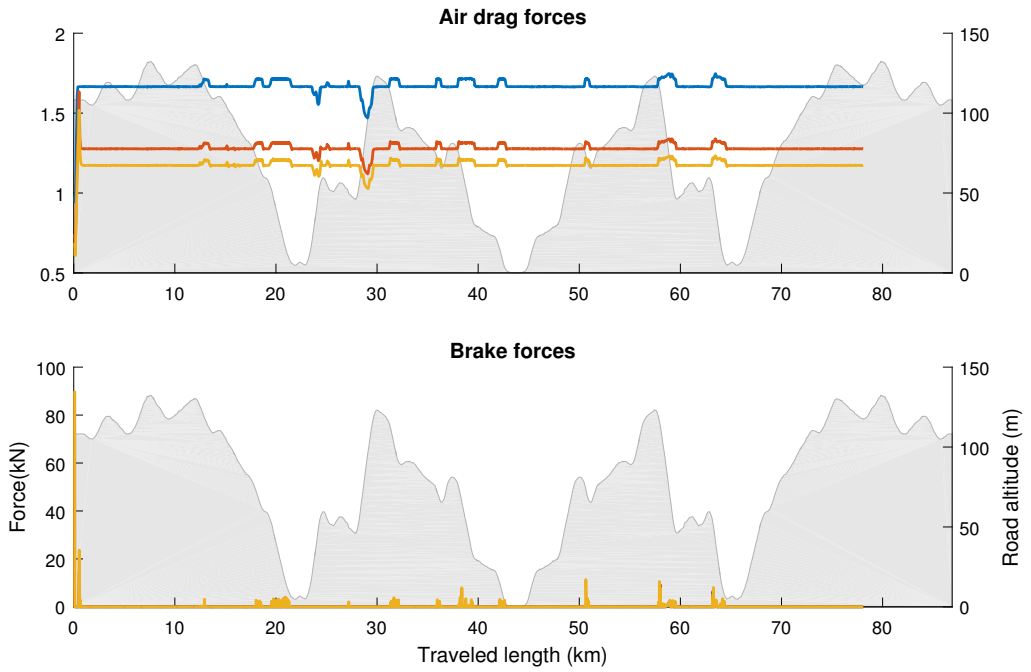

Figure C.1: The air drag and braking forces obtained from the SPC simulation on the BLB drive cycle.

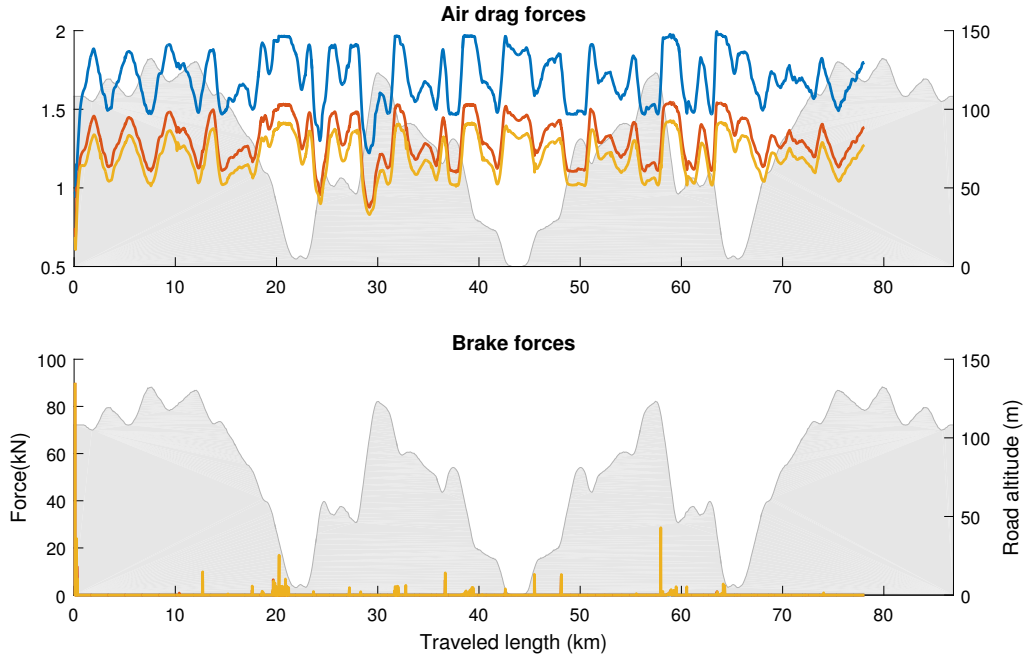

Figure C.2: The air drag and braking forces obtained from the PCC simulation on the BLB road.